QUARTERLY PROGRESS REPORT

PRINCIPLES GOVERNING THE BEHAVIOR OF SOLID MATERIALS IN SEVERE HIGH TEMPERATURE ENVIRONMENTS

June 30, 1965

UNION CARBIDE RESEARCH INSTITUTE

Tarrytown, New York

Project Supervisor Richard W. Kebler

Richard W. Kebler

Submitted by: S. R. Aspinall

S. R. Aspinall, Manager

UC Research Institute

Sponsored by

Army Missile Command

Contract DA-01-021-AMC-11926 (Z)

QUARTERLY PROGRESS REPORT

PRINCIPLES GOVERNING THE BEHAVIOR OF SOLID MATERIALS IN SEVERE HIGH TEMPERATURE ENVIRONMENTS

June 30, 1965

UNION CARBIDE RESEARCH INSTITUTE
Tarrytown, New York

Project Supervisor Richard W. Kebler
Richard W. Kebler

Submitted by: S. R. Aspinall
S. R. Aspinall, Manager
UC Research Institute

Sponsored by
Army Missile Command
Contract DA-01-021-AMC-11926(Z)

FOREWORD

This research program is being carried out in the research laboratories of Union Carbide Corporation located at Tarrytown, New York (Union Carbide Research Institute). The work is supported by the Army Missile Command, Redstone Arsenal, Alabama under Contract No. DA-01-021-AMC-11926(Z). The report period is from March 8, 1965 to June 30, 1965.

The program at Union Carbide Research Institute is supervised by Dr. Richard Kebler with Dr. S. R. Aspinall serving as general project coordinator and Manager of the Institute.

The scope of the program is directed toward understanding the behavior of materials in severe high temperatures characteristic of rocket nozzle environments, learning how to make the most effective use of available materials, and obtaining a better knowledge of optimum properties desired for specific utilization of new materials.

TABLE OF CONTENTS

I. SUMMARY

The reaction between high-density tungsten and H_2O vapor has been studied from 1900 to 2800°K in the induction-heated stagnation-flow reactor at H_2O partial pressures from 25 to 155 torr. The reaction is linear with time at all pressures and temperatures studied. All isobars show apparent activation energies that decrease with temperature, indicating that gas-phase diffusion limits the reaction rates at the higher temperature. Furthermore, the rates are dependent on the gas flow rate at the higher temperatures, consistent with this interpretation.

Rate data previously obtained for the W-CO_2 reaction are being analyzed in terms of a model including diffusion effects, reaction of the oxygen formed by cracking of CO_2, and activated sticking of CO_2 on the tungsten surface; this model employs certain results of the mass-spectrometric studies being conducted here.

Difficulties traceable to the slow reaction of W with HF were encountered in the study of the W-HF reaction in the arc-image stagnation-flow reactor. Reactions due to impurities in the HF and small amounts of air introduced through leaks in the system tend to obscure the desired reaction.

The relative rates of production of gaseous O, WO, and WO_2 by the W-O_2 and W-CO_2 reactions have been studied mass-spectrometrically. Qualitatively, the results are in accord with the assumption that the cracking of CO_2 to give CO(g) and adsorbed oxygen atoms is the rate-controlling step in the W-CO_2 reaction and that, once the oxygen is adsorbed, the reaction proceeds by the mechanism previously deduced for the W-O_2 reaction.

Two tungsten nozzle inserts and holders instrumented with thermocouples were completed. Three ATJ graphite nozzle inserts and holders were sent to the Army Missile Command for initial trials of our holder design and their new test motor.

Further transverse rupture strength (TRS) data confirm the desired behavior of the TaC-Ag skeletal composites. Their room-temperature strength is nearly double that of the self-bonded carbide and TRS compar-

able to that for the self-bonded carbides is maintained at high temperatures. Improved composite strengths were sought by alloying the silver with copper. The high-temperature strengths are maintained but the mechanical properties are no better than those found for silver alone.

Vaporization of silver from and chemical corrosion of TaC-Ag composites and commercial W-Ag composites were studied in the arc-image reactor. Similar self-cooling by vaporization of silver was found for both composites. The corrosion rate of the TaC-Ag composite in CO_2 is comparable to that of dense tungsten and less than that of a commercial W-Ag composite.

Skeletal carbides using Ni as an infiltrant do not maintain their strength at temperatures approaching the melting point of nickel because the bonding between the carbide grains is disrupted by the infiltrated molten nickel. Attempts to "presaturate" the nickel by melting in contact with TaC before infiltration were unsuccessful.

Self-bonded 80 TaC/20 HfC and 80 TaC/20 ZrC alloys were prepared for composite fabrication and their transverse rupture strengths measured; these are high and relatively constant from room temperature to 2000°C.

II INTRODUCTION

This program is concerned with the principles governing high-temperature chemical and physical behavior of refractory materials especially in the respects that may contribute importantly to the successful performance of these materials as rocket nozzle components operating at high temperatures. In this program emphasis will be placed on chemical corrosion since understanding and the ability to predict operational performance are of great importance in making effective use of available materials. Further, guidance can be provided for the selection of the most likely material combinations for new propellant systems.

Recent studies have shown that chemical corrosion is a major cause of nozzle enlargement during firing and that the kinetics of reactions of the corrosive gas species with the insert surface must be known and taken into account in predicting the chemical corrosion of nozzle inserts. Reaction rates between various gases or combinations of gases and possible nozzle materials are being studied as functions of temperature and pressure in this program. However, at typical temperatures for rocket operation these gas-solid reactions may be controlled not by the surface reaction rate but partly or entirely by the rates of diffusion of reactants to the surface or of products away from it. Special efforts are being made to measure truly surface-controlled reaction rates for the various refractory materials at all temperatures of interest by using experimental conditions that afford very high mass-transfer rates. Specialized computer programs for analyzing the experimental data and calculating the corrosion rates in the diffusion-limited and transition regimes are being evolved.

The rate equations developed and our techniques for predicting chemical corrosion behavior of rocket nozzle inserts will be put to the test of predicting the results of actual small test motor firings. The small motor firings are to be carried on at the Army Missile Command, Huntsville, Alabama.

The refractory carbides, which have high melting points and good strength and creep resistance at high temperatures, are potentially important materials for rocket-nozzle construction. Their brittleness and low resistance

to thermal shock, however, have provided strong argument against their development for this purpose. Previous research in this laboratory has indicated skeletal carbide composites, consisting of refractory carbide bodies with continuous fine porosity infiltrated with ductile metals, offer promise of overcoming these limitations. Further improvement of their physical and mechanical properties, as well as resistance to chemical corrosion, is being sought. New compositions and fabrication techniques are being developed. Their strength, ductility, and other properties important for resistance to thermal shock are being measured, along with their resistance to oxidation.

III. TECHNICAL RESULTS AND PLANS

A. Gas-Solid Reactions

Introduction

If the effect of a corrosive environment on a refractory material is to be predicted, rate expressions for the possible chemical reactions must be available from laboratory studies approaching as closely as possible the conditions of temperature and pressure of that environment. However, slowness of gas-phase diffusion can interfere with laboratory measurements, obscuring the surface kinetics, just as it affects the practical situations. Experiments intended to provide surface-kinetic data must therefore be carefully analyzed with respect to gas diffusion and designed to minimize its effects.

Our first objective is the determination of the surface-controlled rates of reactions between gaseous rocket exhaust components and actual or potential rocket nozzle materials in the range of temperatures and pressures characteristic of rocket operations. Our second objective is the development of methods of applying such rate data, in conjunction with aerodynamic analyses, to predict corrosion rates in the transition region between surface and diffusion control. To weigh the extent of control by gaseous diffusion all the data obtained in this program are analyzed to determine where diffusional effects are important.

We have designed and built a number of experimental reactors in which high mass-transfer rates are achieved through use of high velocity gas streams impinging in stagnation patterns on hot samples; the effect for a given reaction is to raise very considerably the temperatures at which gaseous diffusion becomes important in determining observed reaction rates, thus allowing the measurement of purely surface-controlled reaction rates to be made at higher temperatures than otherwise possible. Results obtained in such reactors for the reactions of tungsten with gaseous H_2O, CO_2, and HF are discussed in Sections A-1, 2, and 3, respectively.

The experimental arrangements described above, though capable of yielding rate expressions at temperatures and pressures of direct interest in rocket propulsion, all operate under conditions that preclude observation of the details of the gas-surface reaction mechanisms. To obtain this type of information mass-spectrometric studies of reactions at very low pressures are being conducted; the results obtained by this technique for the CO_2-W reaction are discussed in Section A-4.

We plan to test the applicability of our models for predicting corrosion rates by comparing predicted with actual nozzle insert corrosion rates. The status of this program is discussed in Section A-5.

1. Kinetics of the Tungsten-H_2O Reaction J. M. Quets, P. N. Walsh

This reaction is being studied at temperatures above 2000°K in the induction-heated stagnation-flow reactor shown schematically in Fig. A-1, which was previously used in the study of the CO_2-tungsten reaction (cf. Section A-2). The sample is a tungsten cylinder, 3/4" in diameter by 1/2" in height, mounted by a slip-fit onto a 1/8" diameter tungsten rod supported from the bottom of the reactor. The sample is heated inductively; coupling to the induction coil mounted outside the Pyrex glass envelope is achieved through use of the 1" i.d. water-cooled-copper current concentrator. Temperatures in excess of 3000°K have been obtained. The reactive gas is brought in through the 1/4" i.d. water-cooled copper tube, the outlet of which is mounted 1/4" from the sample surface. The reactive gas impinges normally on the sample surface forming a stagnation pattern in which the highest gas-solid mass transfer rate occurs at the stagnation point. The recession of the sample surface is measured at this point. The reaction rate is given directly by depth of removal of tungsten divided by the reaction time; this rate is ordinarily converted to moles cm^{-2} sec^{-1} by multiplying by the ratio of the density of tungsten to its atomic weight.

The sample is preheated and cooled in argon to eliminate any possible "edge effects" that might be occasioned by reaction during heating up and cooling down. The reaction mixture is admitted only after the temperature has been stabilized; solenoid valves and an associated timer limit this flow to the desired time. The gases are continuously pumped out through the bottom of the concentrator: constant pressure at any level below atmospheric is obtained by controlling the rates of input and removal of the gases. The pressure of interest is the stagnation pressure at the stagnation point which can be calculated assuming a compressible isentropic flow of perfect gas. Pressure probes, operated both at room temperature and in excess of 2000°K, placed at the sample position have verified the validity of this assumption.[1]

The temperature at the stagnation point is measured during the reaction by an optical pyrometer sighted down the gas inlet tube through a totally-internal-reflecting prism. Corrections for the absorptivity of the window and prism and for the emissivity of the tungsten surface are

made to obtain sample surface temperatures. At the temperatures of this study all the reaction products are volatile and are continuously removed from the tungsten surface. These products condense to a fog a short distance from the surface, but the gas flow sweeps them out of the line of sight of the pyrometer. It has been shown previously[1] that under these conditions the emissivity of the tungsten surface during reaction does not differ significantly from that of smooth polished tungsten.

Water vapor is provided by a steam generator fed by deoxygenated distilled water. After passing through a calibrated critical flow orifice meter it is mixed with a measured flow of argon, which has been preheated to about 80°C, and the mixture is then introduced into the gas inlet tube. With a total flow of 100 standard liters/minute (SLM) of water vapor-argon mixture through the 1/4" nozzle, the gas velocity is approximately 1.3×10^4 cm/sec. With a total static pressure of 300 torr in the reaction chamber, the stagnation total pressure at the tungsten surface is approximately 340 torr. The partial pressures of water vapor reported here were calculated from the stagnation pressure and the fraction of water vapor in the reacting mixture.

Recession rates have been obtained at six water vapor partial pressures. The recession of the tungsten surface at the stagnation point was found to increase linearly with time at every temperature and partial pressure investigated; typical data are shown in Figs. A-2 and A-3. All the recession rates are plotted in Fig. A-4 to A-9 as log of recession rate (in moles cm^{-2} sec^{-1}) vs. inverse absolute temperature and summarized in Fig. A-10. For each partial pressure the data shows the same characteristic: The apparent activation energy is approximately 60 kcal/mole at low temperature, and decreases as the temperature increases.

No attempt to fit the data to a model has been made, but it seems likely that diffusion through the boundary layer becoming increasingly important at higher temperature is largely responsible for the curvature in the log rate vs. 1/T plots. To check on this, data were taken with a total flow of reacting gas mixture of 10 SLM (Fig. A-9). The reaction rates scattered widely because of difficulty in controlling low steam flows through the critical flow orifice. Nevertheless, it is clear that a constant oxidation rate is approached at the highest temperature as expected if the reaction rate becomes completely determined by gaseous diffusion rates.

Plots of log rate vs. log P_{H_2O} (Fig. A-11) indicate that the apparent order in free-stream H_2O pressure decreases from about 0.9 near 2000°K to about 0.7 near 2800°K. These plots suggest that the data obtained with 93 torr H_2O are systematically in error. There is also a suggestion that the apparent order may be pressure dependent at the lower temperatures.

Difficulties in maintaining constant higher temperatures, caused partly by the deposition of reaction products between the concentrator wall and the sample, have effectively limited the temperature range to an upper value of approximately 2800°K.

Future Work

During the next quarter, hydrogen will be added to the reacting gas mixture in increasing amounts. Also, additional data will be taken using a low flow of reactive gases.

Ways will be sought to overcome the difficulties encountered in maintaining constant higher temperatures in order to increase the useful temperature range.

References

1. "Kinetics of the Tungsten-CO_2 Reaction above 2000°K", P. N. Walsh, J. M. Quets, R. A. Graff and I. R. Ladd, Appendix to Final Report on Contract DA-30-069-ORD-2787, ARPA Order No. 34-63, Task 4.

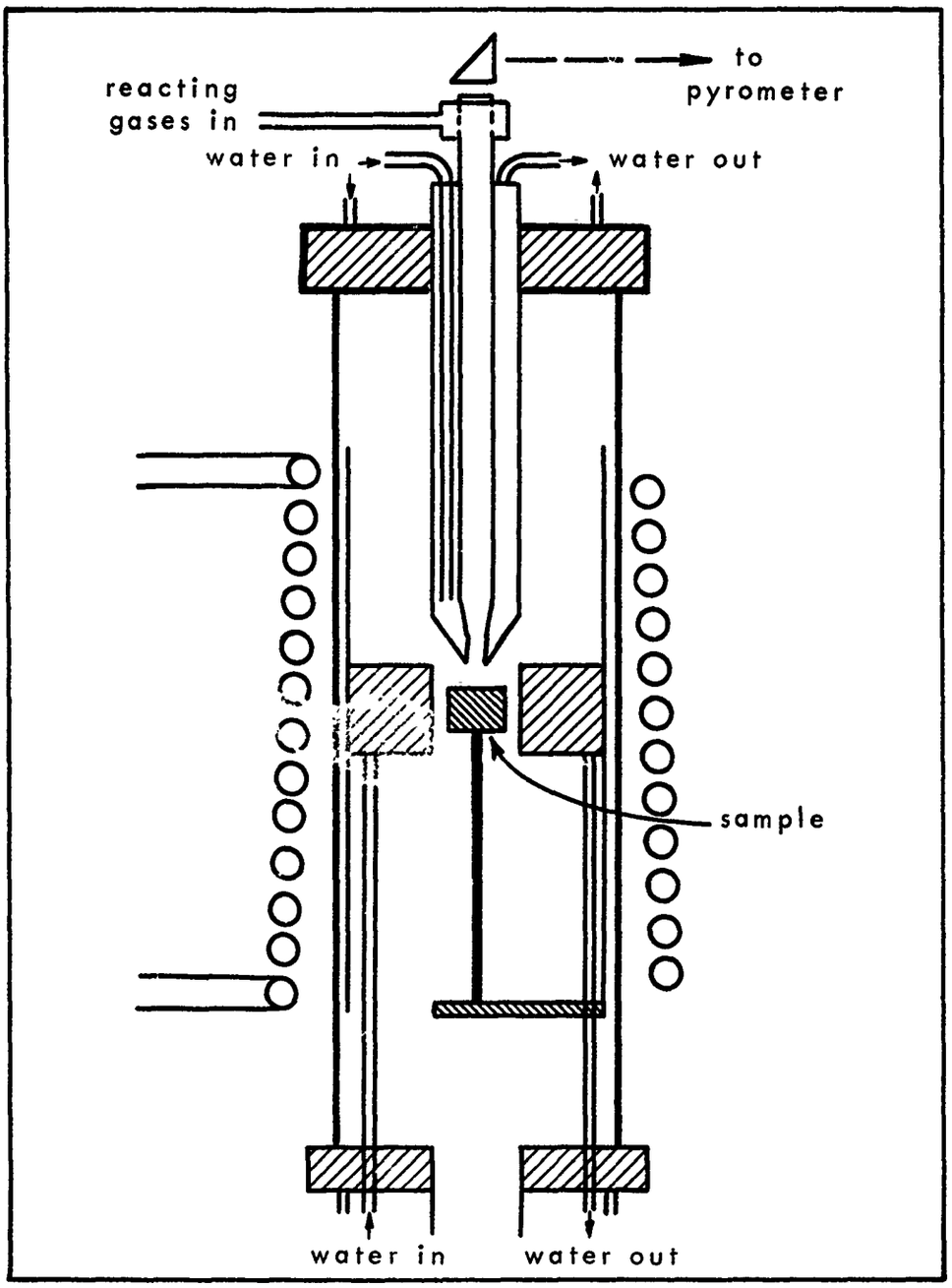

FIGURE A - 1 SCHEMATIC OF STAGNATION FLOW REACTOR

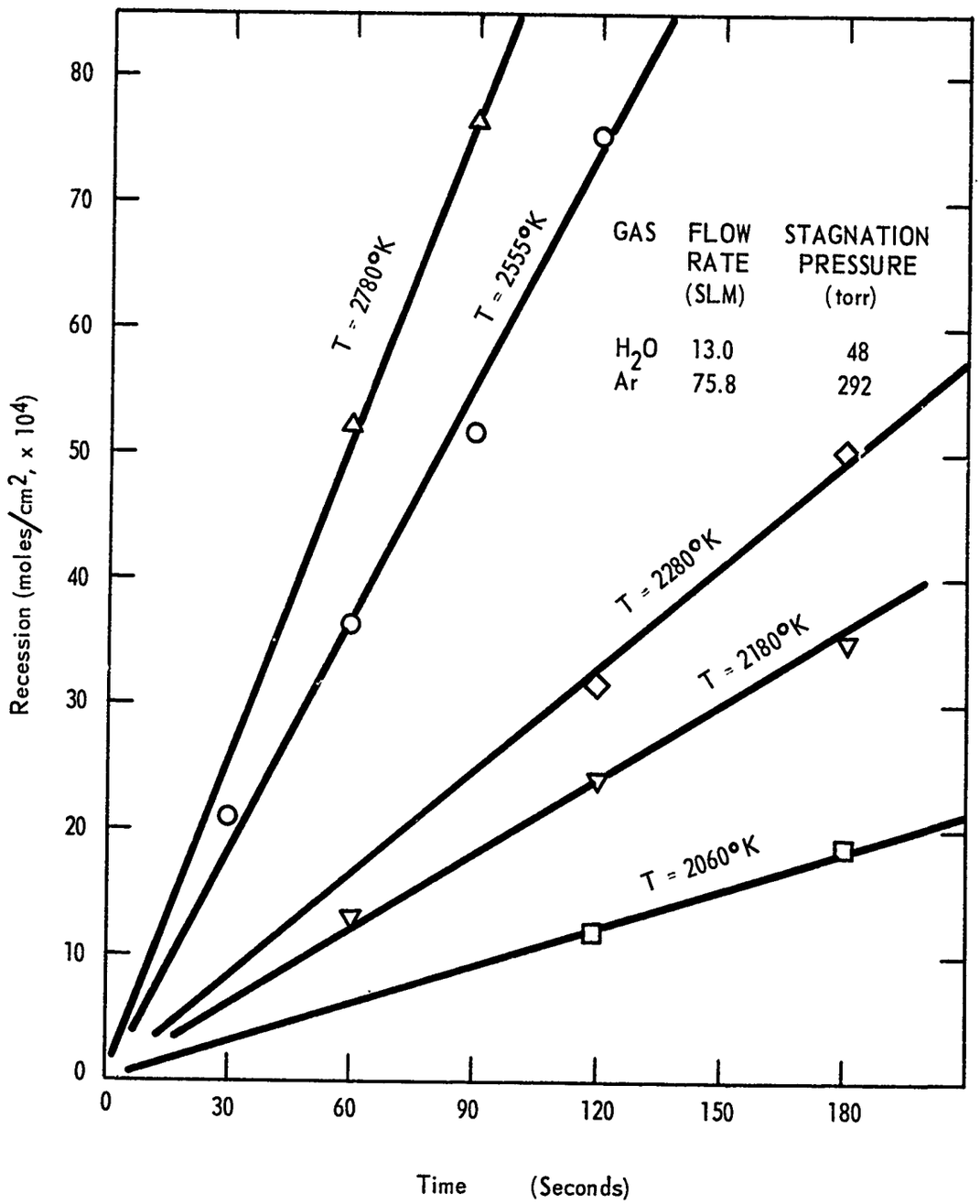

FIGURE A - 2 TIME DEPENDENCE OF RECESSION OF TUNGSTEN AT SEVERAL TEMPERATURES

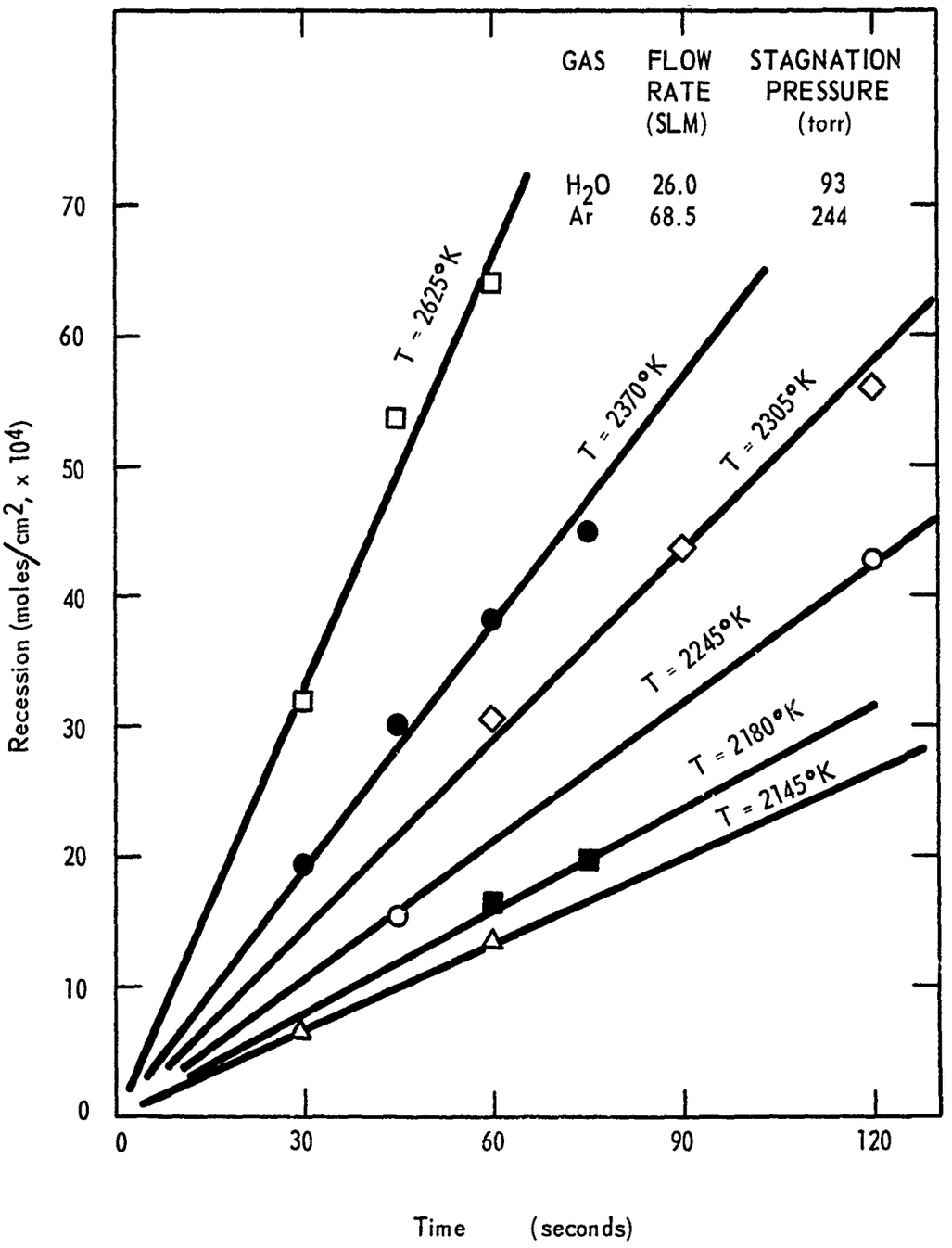

FIGURE A - 3 TIME DEPENDENCE OF RECESSION OF TUNGSTEN AT SEVERAL TEMPERATURES

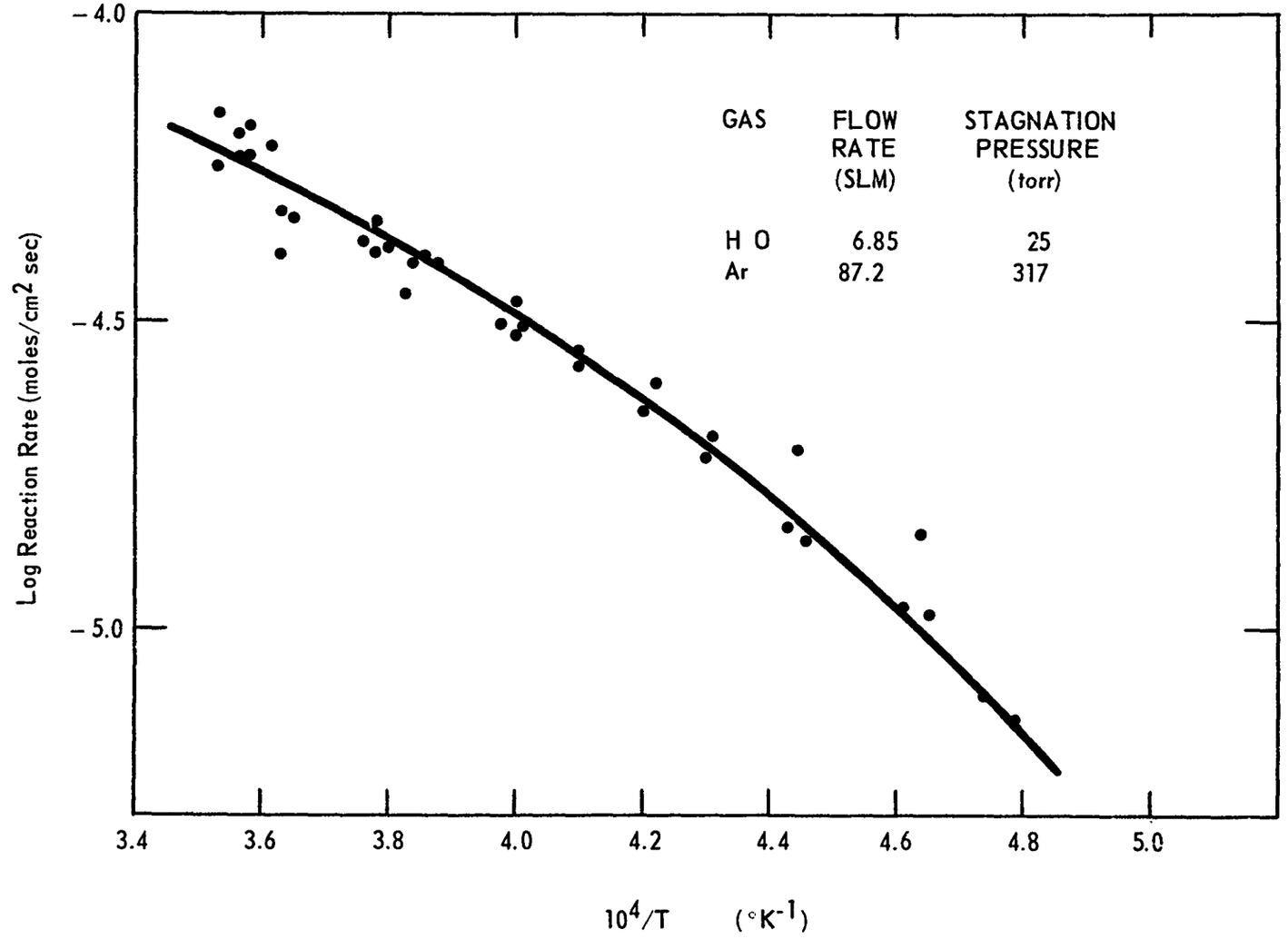

FIGURE A - 4 TEMPERATURE DEPENDENCE OF RATE OF W-H_2O REACTION –25 TORR H_2O

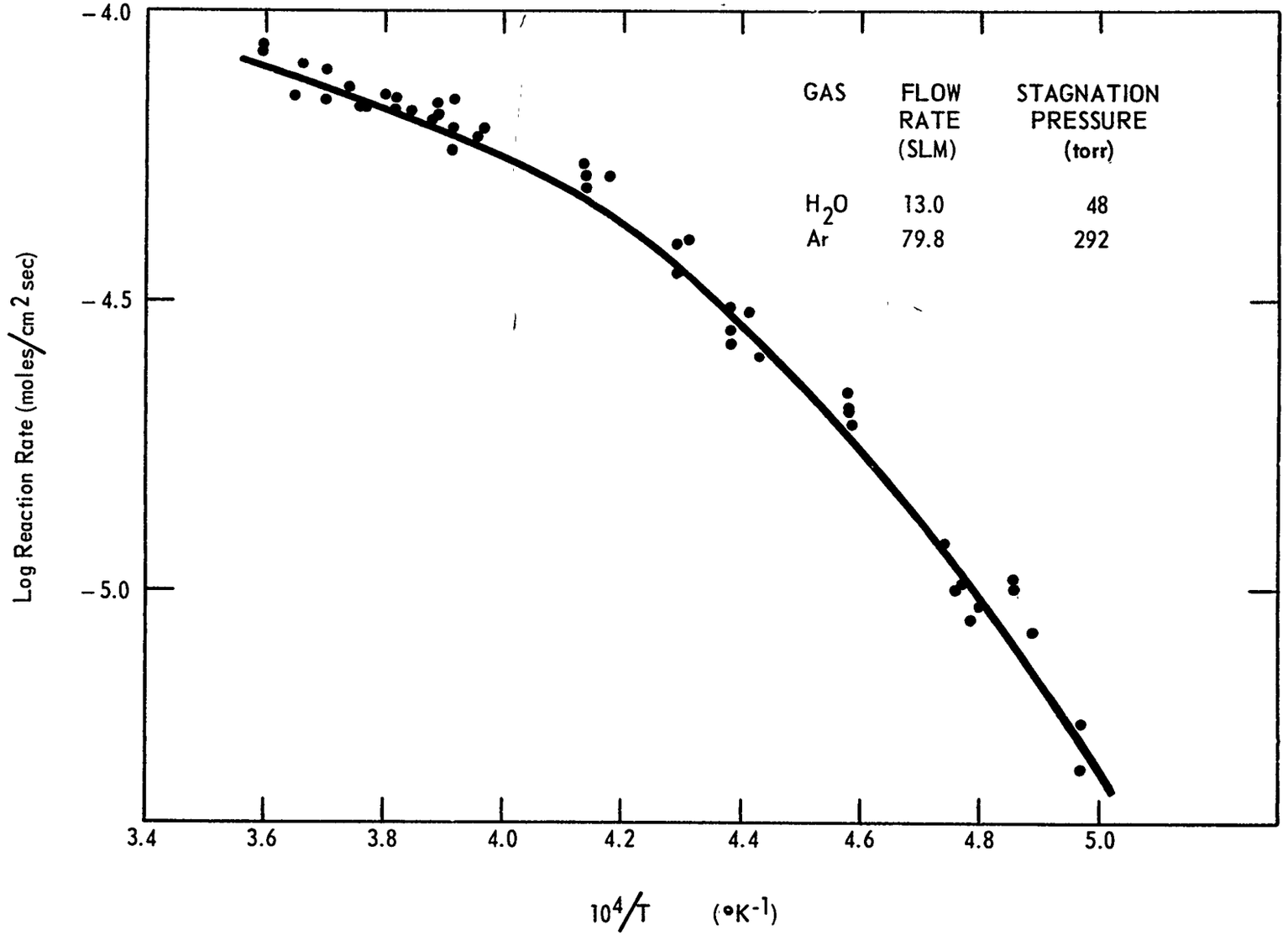

FIGURE A - 5 TEMPERATURE DEPENDENCE OF RATE OF W-H_2O REACTION –48 TORR H_2O

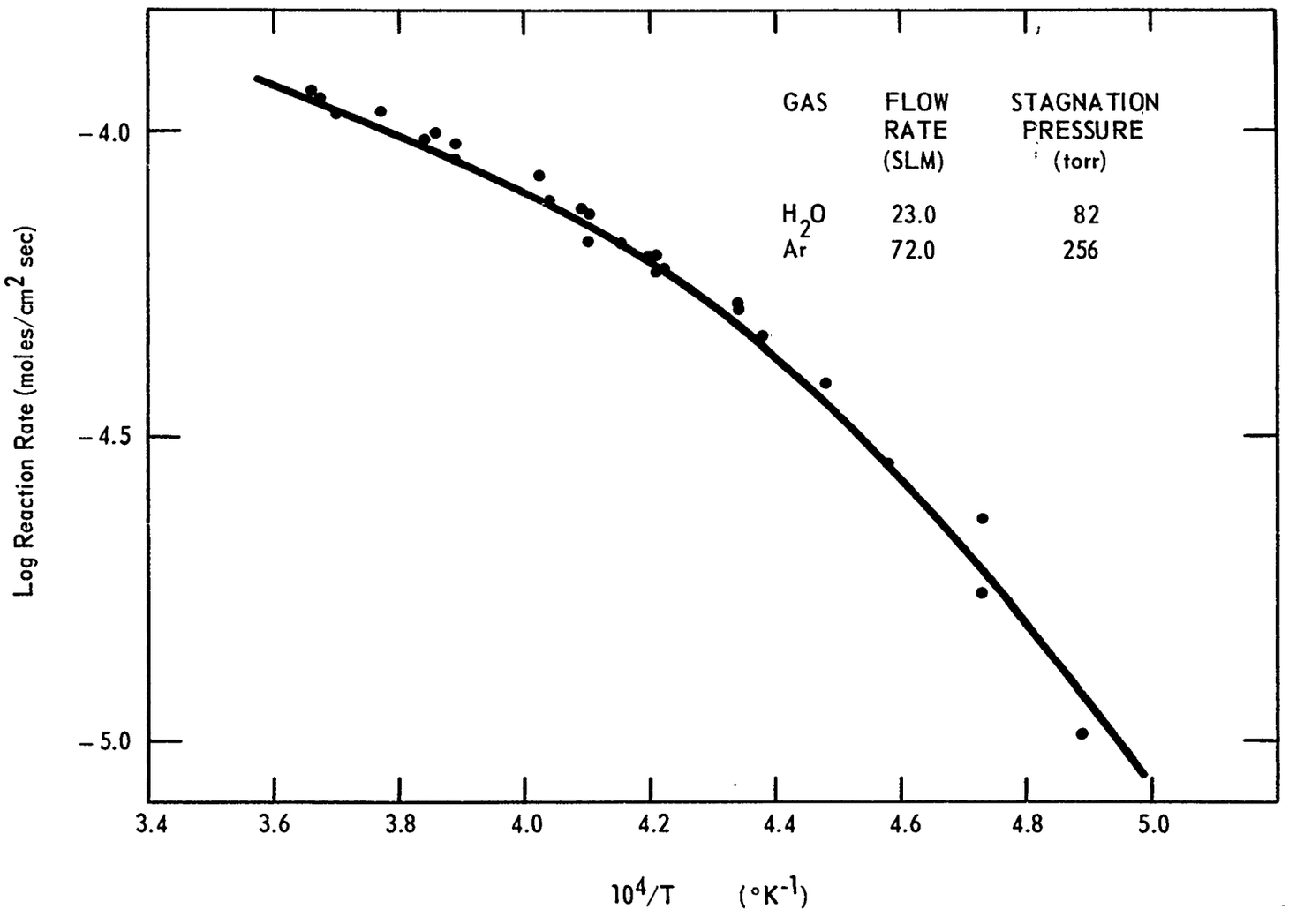

FIGURE A - 6 TEMPERATURE DEPENDENCE OF RATE OF W-H_2O REACTION –82 TORR H_2O

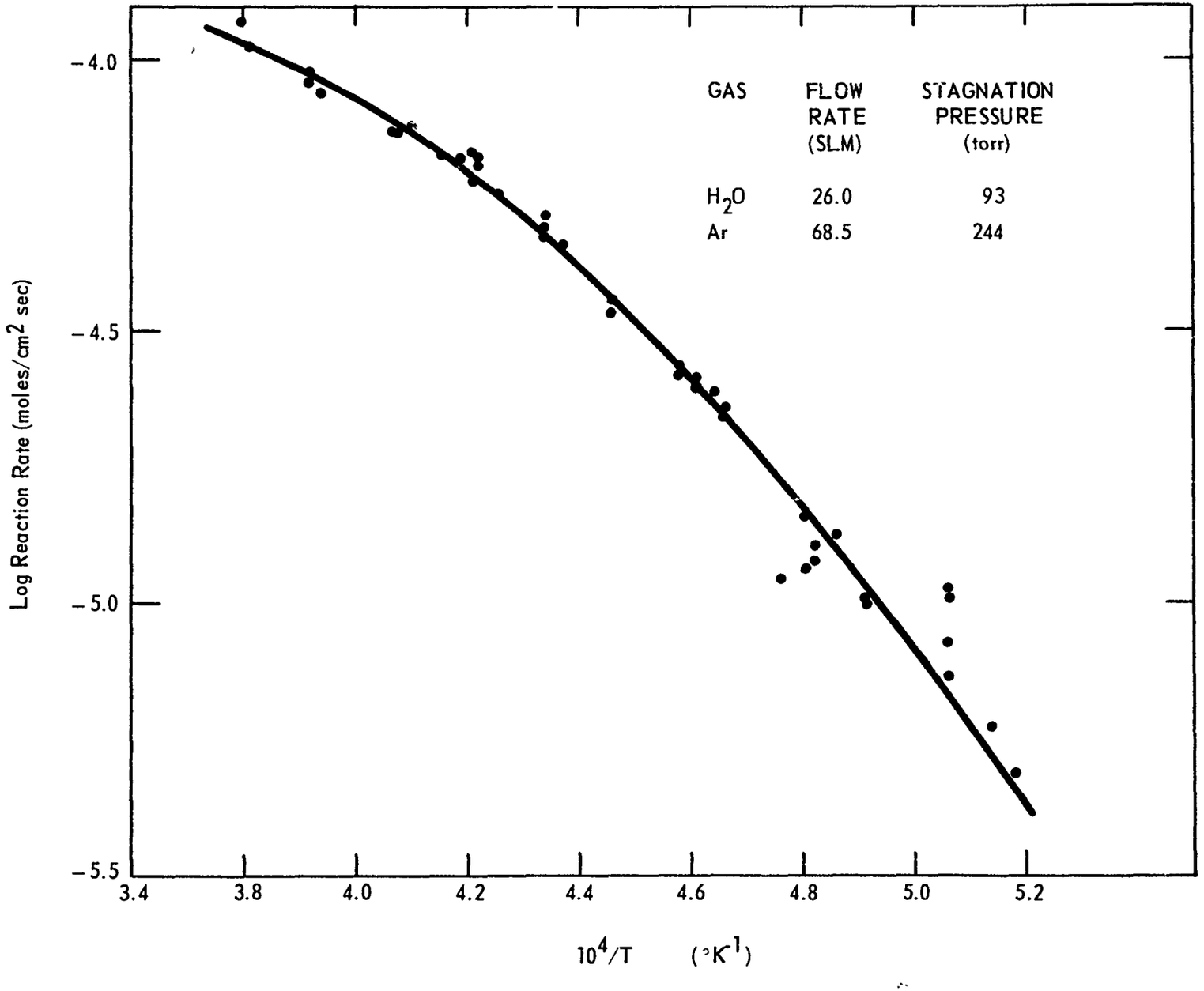

FIGURE A - 7 TEMPERATURE DEPENDENCE OF RATE OF W-H_2O REACTION –93 TORR H_2O

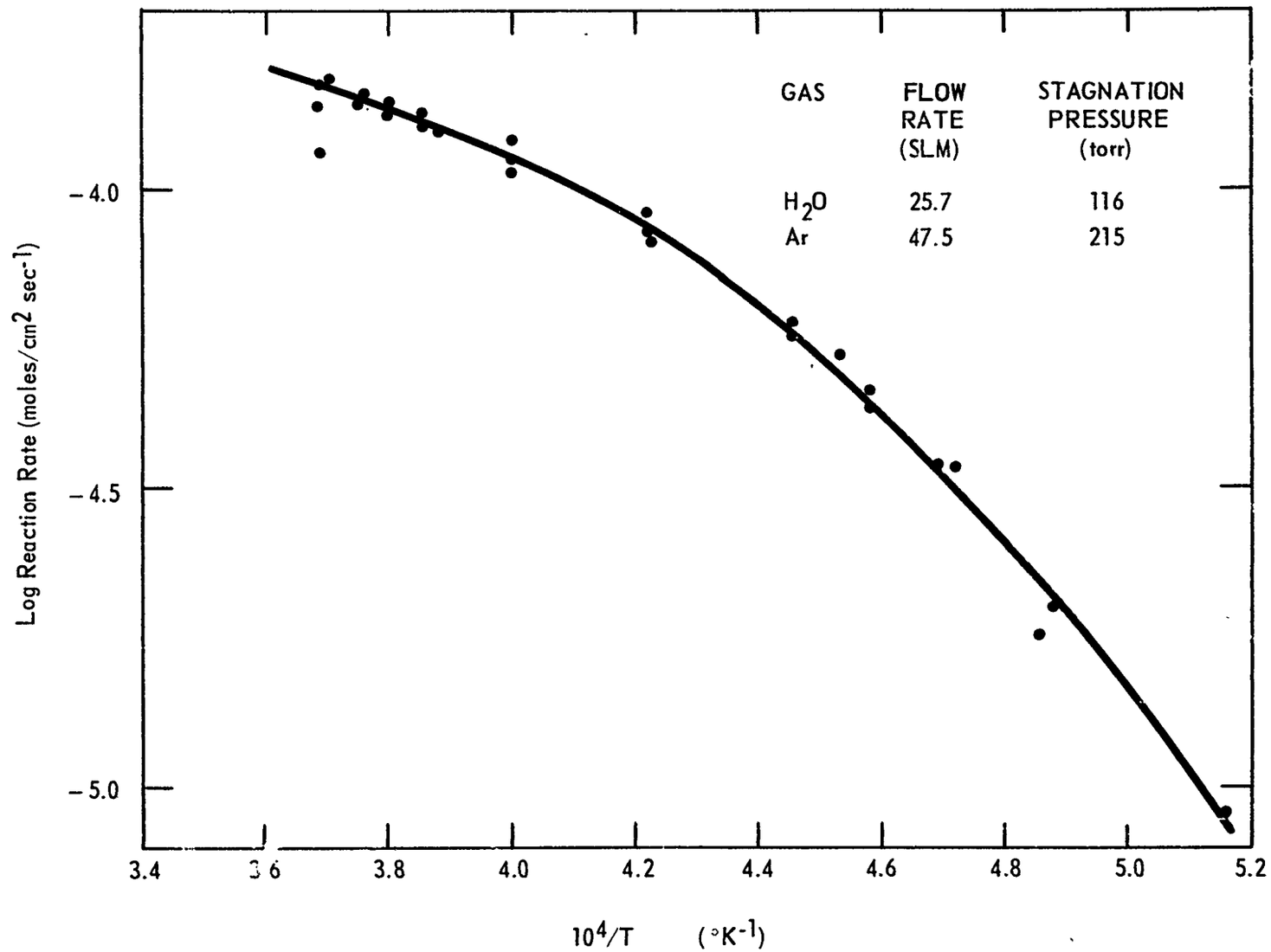

FIGURE A - 8 TEMPERATURE DEPENDENCE OF RATE OF W - H_2O REACTION –116 TORR H_2O

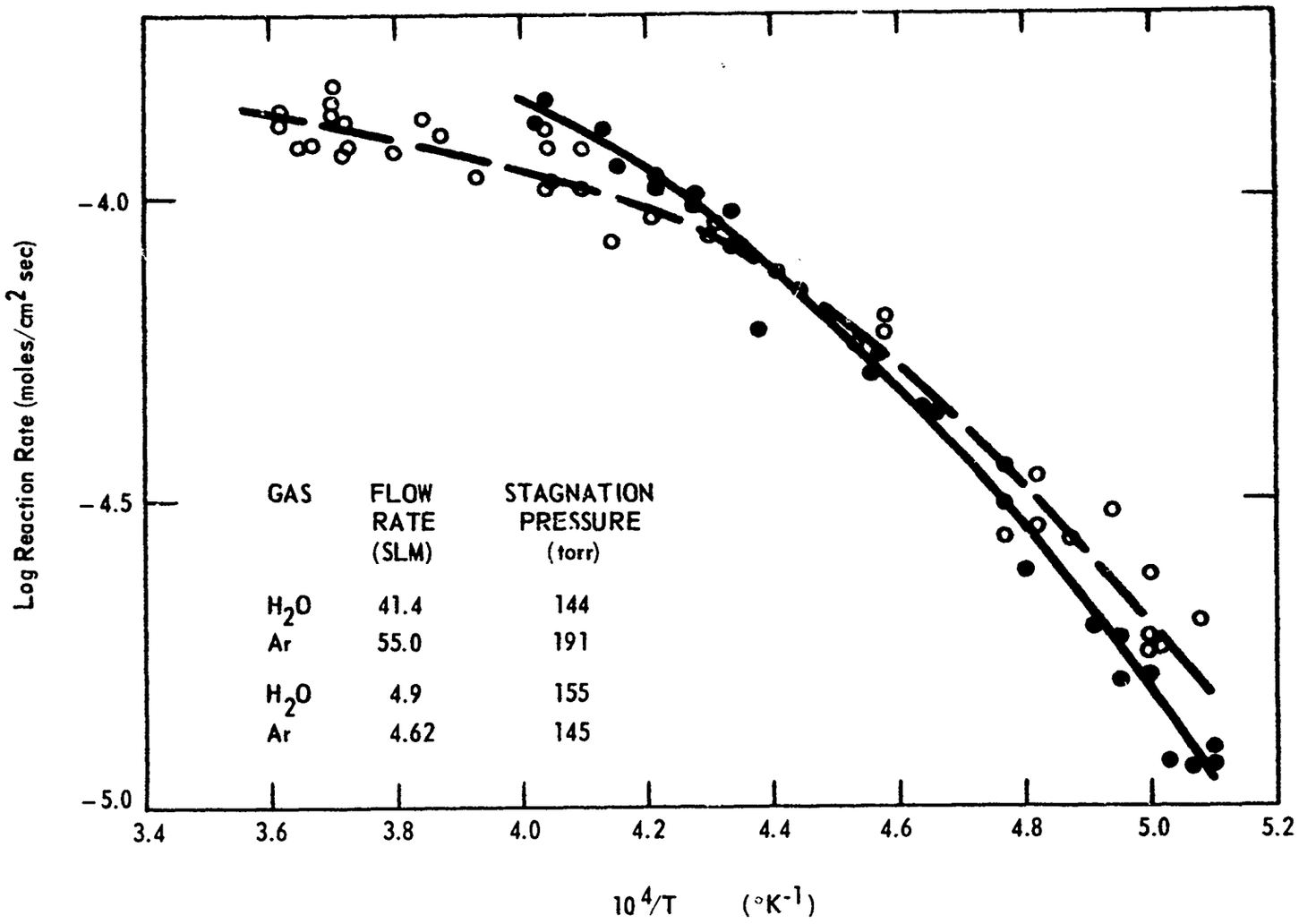

FIGURE A - 9 TEMPERATURE DEPENDENCE OF RATE OF W-H_2O REACTION AT TWO FLOW RATES

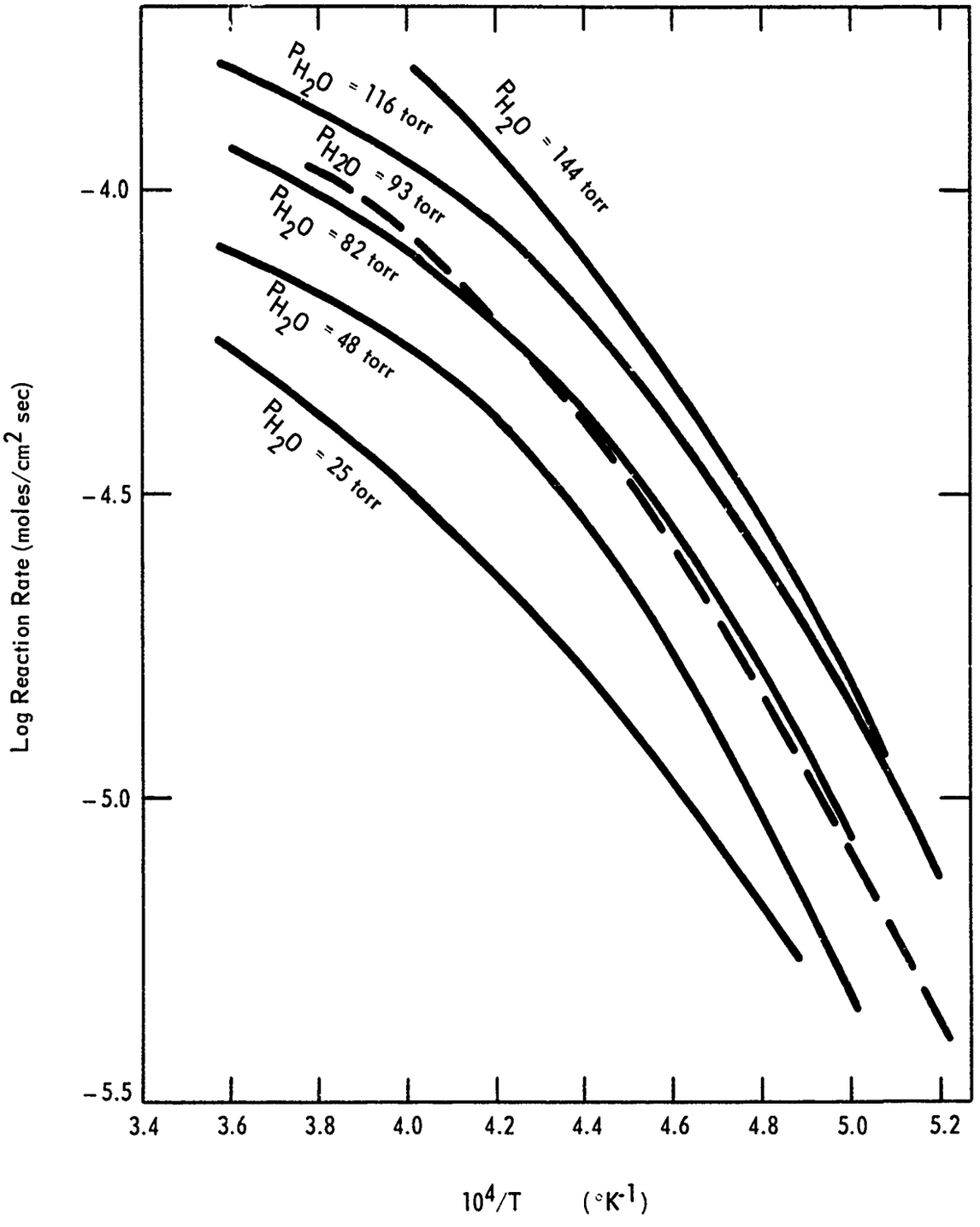

FIGURE A - 10 TEMPERATURE DEPENDENCE OF RATE OF W-H_2O REACTION AT SEVERAL PARTIAL PRESSURES

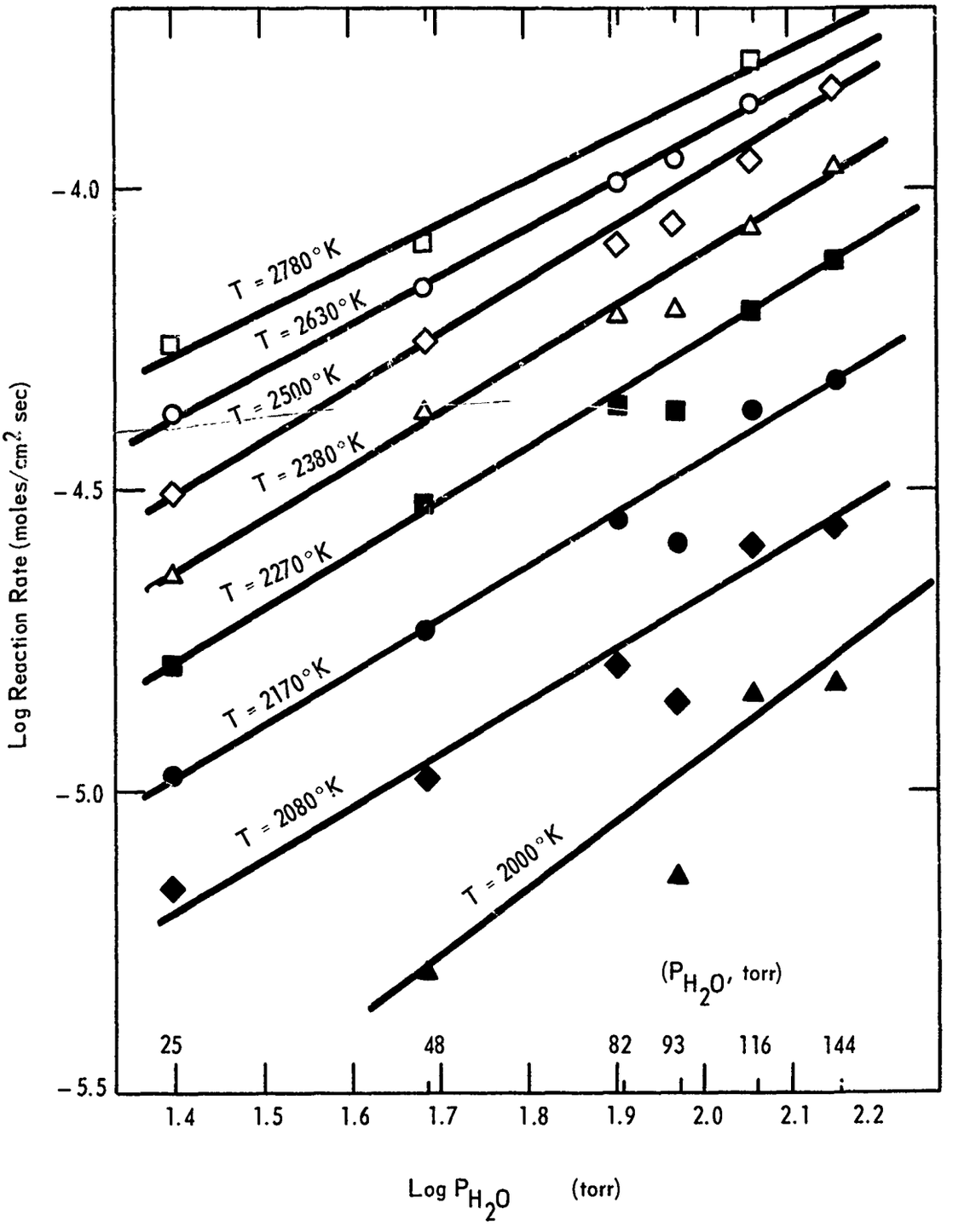

FIGURE A - 11 PRESSURE DEPENDENCE OF RATE OF W-H_2O REACTION AT SEVERAL TEMPERATURES

2. Kinetics of the W-CO_2 Reaction

J. M. Quets, P. N. Walsh, and R. A. Graff

This reaction was extensively studied, in the stagnation-flow reactor described in Section A-1, under Contract DA-30-069-ORD-2787. The rates and temperature dependences obtained for CO_2/Ar and CO_2/CO/Ar gas mixtures are summarized in Figs. A-12 and A-13, respectively. The data may be found in previous reports.[1,2] No completely successful interpretation of the kinetics was developed under the previous contract, so analysis of the data has been continued.

Any model for the mechanism of the W-CO_2 reaction must include the following points.

1. The dependence of the higher-temperature reaction rates (Fig. A-12) on the rate of flow of the incoming gas shows that diffusion of reactants and products in the gas phase becomes important in determining the reaction rates at these temperatures. The model therefore must account for diffusion effects. Since complete diffusion control, corresponding to gas-solid thermochemical equilibrium, is apparently achieved under some conditions, e.g., curve 1, Fig. A-12, the model must include equilibrium as a limit.

2. The reaction is inhibited, but only slightly so, by CO; compare curves 1 and 2 or curves 4, 5, and 6 in Fig. A-13.

3. Mass-spectrometric studies (Section A-4) have shown that CO_2 is cracked by hot W to produce gaseous O and O_2 and suggest that the sticking of CO_2 on W is activated. At pressures near one-half atmosphere, the O and O_2 cannot rapidly escape the vicinity of the reacting surface, so their return to the surface must be considered.

4. The reaction is nearly first-order in free-stream CO_2 pressure even at the lowest temperatures.

These conditions and the reported mechanism of the W-O_2 reaction,[3] suggest that, as a minimum, the following reactions be included:

$$CO_2(g) + n\,S \underset{k_1}{\overset{\sigma_1\nu_1}{\rightleftharpoons}} CO(g) + O^* + (n-1)S \qquad (1)$$

$$2\,O^* \underset{\sigma_5\,\nu_5}{\overset{k_2}{\rightleftharpoons}} O_2(g) + 2\,S \qquad (2)$$

$$O^* \underset{\sigma_4\nu_4}{\overset{k_3}{\rightleftharpoons}} O(g) + S \qquad (3)$$

$$m\,O^* + M \underset{\sigma_2\nu_2}{\overset{k_4}{\rightleftharpoons}} WO_x(g) + m'S \qquad (4)$$

In reactions 1-4, S signifies a site taken to be a "second layer" site in terms of the model of reference 3; in the same terms, O^* is a second layer adsorbed oxygen atom and M, the entity that combines with O^* to give (reaction 4) tungsten oxide, would be a complex of a first layer adatom and a tungsten atom. For convenience in the computer calculations associated with this problem, the gases have been numbered: CO_2 is 1; WO_x, 2; CO, 3; O, 4; O_2, 5; and Ar, used in the experiments, 6. This numbering has carried over into the rate constants in reactions 1-4: σ_i and ν_i are respectively the (possibly temperature-dependent) sticking coefficients and the kinetic-theory impingement rate of species i. The rate constants involving adatoms, k_{1-4}, follow to an extent the numbering of reference (3), where values for k_2 and k_3 are given; k_4 would be, in the present less-detailed model, the sum of the rate constants k_4 and k_5 of reference (3) for the formation of $WO_2(g)$ and $WO_3(g)$.

The rate constants are related thermodynamically:

$$K_1 = (\sigma_1\nu_1)^2\, k_2/k_1^2\, \sigma_5\nu_5 \qquad (5)$$

$$K_2 = \sigma_1\nu_1 k_3/k_1\sigma_4\nu_4 \qquad (6)$$

$$K_3 = (\sigma_1\nu_1)^x\, k_4/\sigma_2\nu_2 k_1^{\,x} \qquad (7)$$

Here K_1, K_2, and K_3 are respectively the equilibrium constants for reactions 8, 9, and 10.

$$2\,CO_2(g) \rightleftharpoons 2\,CO(g) + O_2(g) \qquad (8)$$

$$CO_2(g) \rightleftharpoons CO(g) + O(g) \qquad (9)$$

$$x\ CO_2(g) + W(c) \rightleftharpoons x\ CO(g) + WO_x(g) \qquad (10)$$

The number of sites involved in reaction 1 is not known. We have so far considered only cases involving n = 1 or n = 2. Gaseous CO is presumed to be in equilibrium with the surface layer, as is the gaseous product WO_x. The product leaving the surface is probably either $WO_3(g)$ or $WO_2(g)$,[3] but gas-phase polymerization to the thermodynamically favored $W_3O_9(g)$ is a possible complication; at the diffusion limit, $W_3O_9(g)$ should be the primary W-O species.

The diffusion of reactant and product gases to and away from the surface is being treated by use of a film model for mass transfer similar to that previously employed for the analysis of diffusion-controlled reactions.[4] In this model the rate of transfer r_j of the jth species across the boundary layer is given by

$$r_j = \tilde{k}_j\ (P_{j\infty} - P_{jw}). \qquad (11)$$

Here, $\tilde{k}_j$ is a mass transfer coefficient, calculated from the hydrodynamic conditions of the experiment and the properties of the gaseous molecules,[4] $P_{j\infty}$ is the free-stream (input) partial pressure of j and P_{jw} its partial pressure at the reacting surface. The reaction rate at the surface depends on the surface partial pressures, and the r_j are fixed by the rate of tungsten consumption and the requirements of mass-balance. Hence the partial pressures that appear in the expression describing the surface kinetics must also satisfy Eq. 11.

No completely successful model has been developed as yet. The approximation that a steady-state concentration of O^*, governed by reactions 1-4, is established appears useful but difficulty has been encountered in finding an appropriate set of constants to explain all the observations. The mass-spectrometric results (reference 3 and Section A-4 of this report) are being used as guides to the proper values of k_2, k_3, and σ_1; values finally chosen will be subject to the test of being compatible with the mass-spectrometric data. Explanation of the extreme sharpness of the transition to diffusion control in curves 1, 3, 5, and 7 of Fig. A-12 has been a major stumbling block.

Future Work

The analysis of the CO_2-W reaction kinetics will be pushed to completion. The results should be pertinent to the understanding of the kinetics of oxidation of tungsten by any oxidizing gas.

To aid in the analysis, data on the O_2-W reaction over a limited range of conditions will be taken in the stagnation-flow reactor.

References

1. Quarterly Progress Reports, March-December, 1964, on Contract DA-30-069-ORD-2787, "Research on Physical and Chemical Principles Affecting High-Temperature Materials for Rocket Nozzles."

2. Final Report, same Contract; to be issued.

3. P. O. Schissel and O. C. Trulson, "Mass Spectrometric Study of the Oxidation of Tungsten," Technical Report No. C-26, Contract DA-30-069-ORD-2787, October 1964.

4. P. N. Walsh and R. A. Graff, "An Algorithm for the Computation of Diffusion-Controlled Rates of Gas-Solid Reactions," Technical Report No. C-30, Contract DA-30-069-ORD-2787, to be issued. Also Quarterly Progress Reports, September, 1963 - June 1964, on the same contract.

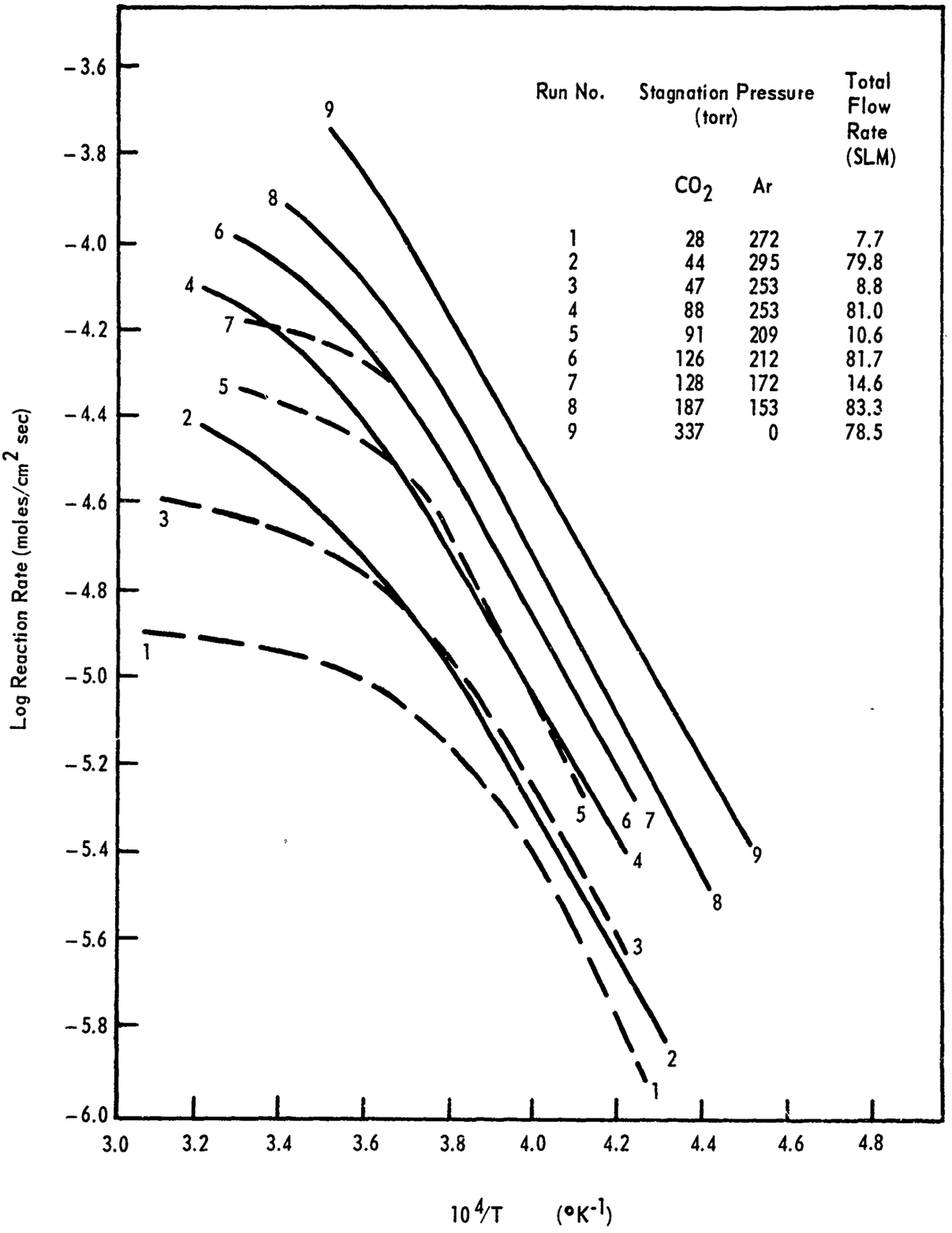

FIGURE A - 12 RATES OF REACTION OF W WITH CO_2/Ar MIXTURES

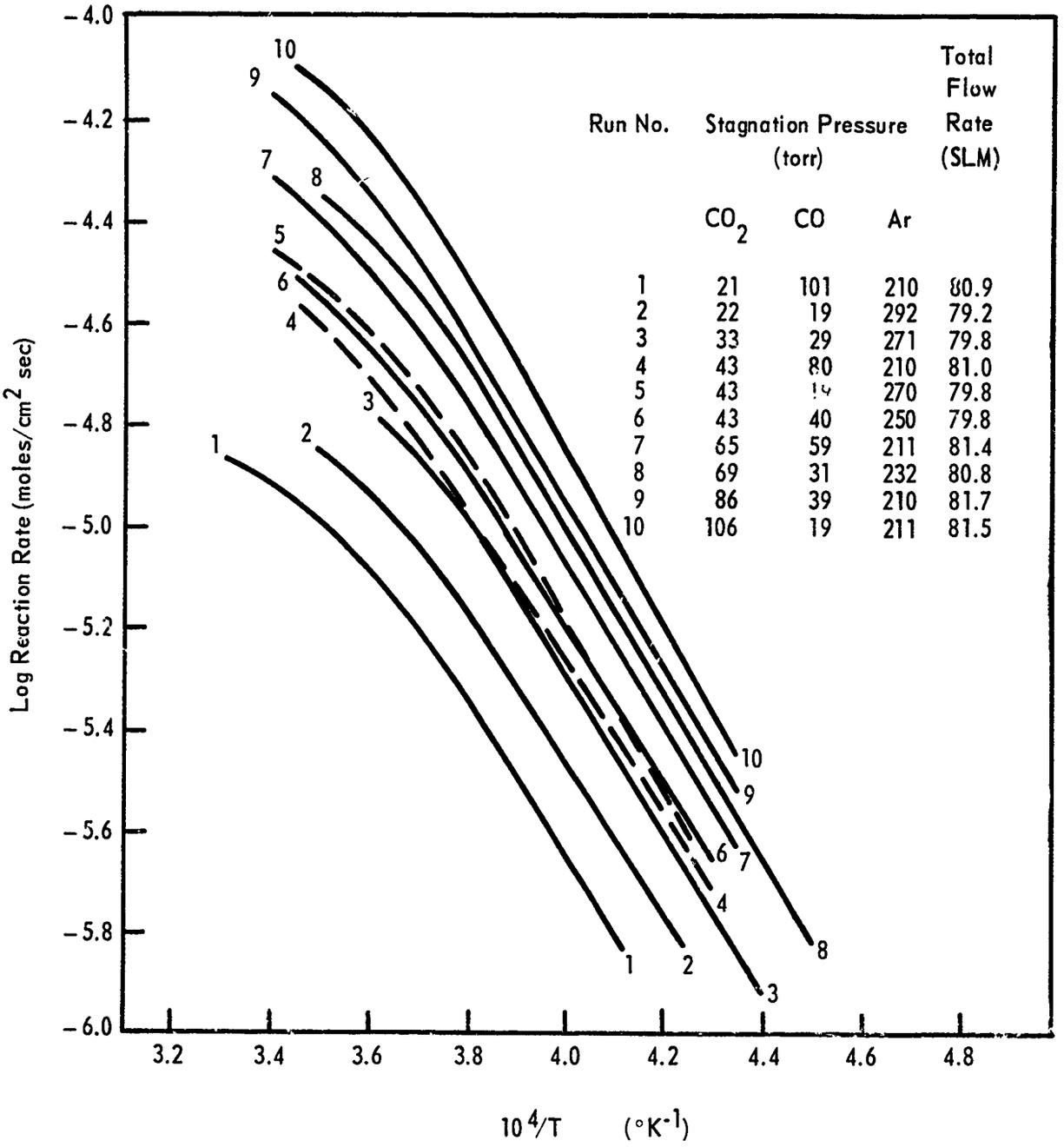

FIGURE A - 13 RATES OF REACTION OF W WITH CO_2/CO/Ar MIXTURES

3. Kinetics of the HF-W Reaction — I. R. Ladd, P. N. Walsh

This reaction has been studied in the arc-image stagnation-flow reactor (Fig. A-14) which is similar in principle to the induction-heated reactor described in Section A-1 in that a controlled flow of reactant gas impinges normal to a preheated solid surface. A technical report describing the reactor is to be issued soon.

The HF gas (99.9% pure, max. 0.04% H_2O) was obtained from a supply cylinder which was immersed to its neck in a 50°C constant temperature water bath in order to maintain cylinder pressure above 20 psig and had its diaphragm valve preheated to prevent irregular surging of HF through the system. The gaseous HF was transported via heated lines to a calibrated critical-orifice meter, then to the reactor nozzle, where it mixed with argon, passed through the nozzle, and struck the sample surface. The HF, Ar and reaction products were mechanically pumped out of the reactor bulb, through a sodium fluoride trap, into a hood. Except for the reactor bulb, all-metal construction was used because the products of the HF-glass reaction caused the oil pump to seize.

If the HF contacts the glass reactor bulb it will rapidly etch it, reducing the transmission of radiation from the arc so that the specimen temperature cannot be controlled. To prevent this, the injector nozzle used with HF produces a high velocity argon sheath around the HF-Ar flow. This sheath flow was adjusted to minimize attack on the bulb in the radiation-transmission area; as a result, temperature constancy was not a problem.

The data obtained (Fig. A-15) were not consistent. They do, however, clearly show HF to be much less corrosive toward W than either CO_2 or H_2O, (cf. Sec. A-1 and A-2) particularly at the higher temperatures studied. In fact, curve C, Fig. A-15, corresponds roughly to what is predicted for the H_2O-W reaction alone on extrapolating data of Section A-1 to the H_2O partial pressure in our HF. The five-fold difference between curves B and C, which should be identical, may have been caused by a small air leak in the argon purge line during run B. Such air leaks are especially serious because of the low reactivity of HF with tungsten, and further confirmation of the rates is needed. The difference between curves D and C may in-

dicate a dependence on gas velocity (diffusion-limited reaction), but in view of the difficulties cited this is far from certain. Microscopic examination of the tungsten samples (v.i.) after reaction strongly suggests a surface controlled reaction. The available thermodynamic data on W-F compounds is insufficient to permit an analytical prediction of the diffusion limit for this reaction.[1]

The low reactivity of W with HF constitutes a serious handicap to the development of good kinetic data in other ways as well. The constant uncertainty in the micrometer measurements of recession, 0.002 mm, corresponds to an uncertainty in reaction rate varying from more than 100% in curve C to 3% in curve A (Fig. A-15). Furthermore, microscopic examination of the reacted surfaces shows that individual crystal grains react at different rates. In several cases the difference in height of nearby grains was one-third as great as the macroscopically measured recession.

Future Work

Further attempts to measure W-HF reaction rates will be made next quarter. Study of the Ta-HF reaction will be initiated as a preliminary to a TaC-HF reaction investigation. The comparative inertness of the graphite holders in the work already done clearly demonstrates that, as expected, the rate of HF attack on graphite will be too small to measure accurately. The arc-image reactor will also be used for further studies of the CO_2-ZrC and CO_2-TaC reactions.

References

1. Quarterly Progress Report, Research on Physical and Chemical Principles Affecting High-Temperature Materials for Rocket Nozzles, June 1964, Contract No. DA-30-069-ORD-2787.

2. Ibid, December 1964.

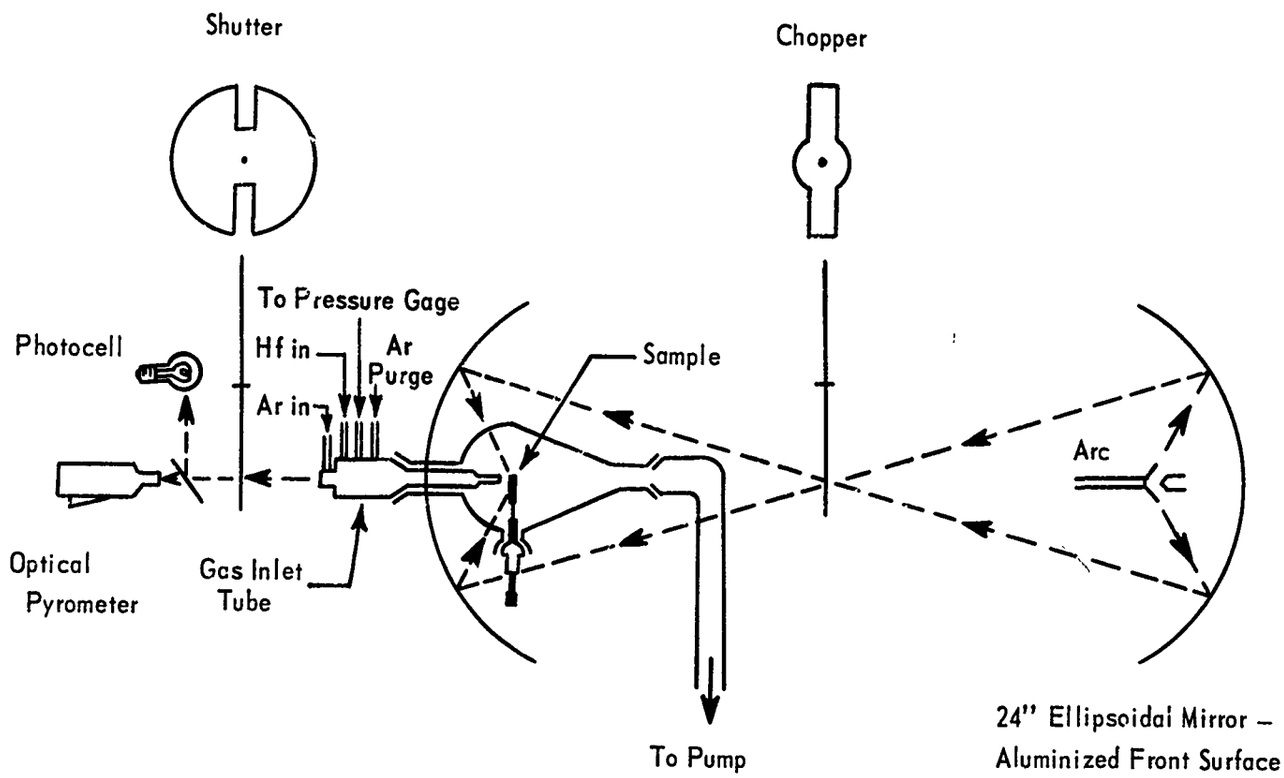

FIGURE A - 14 ARC-IMAGE STAGNATION-FLOW REACTOR

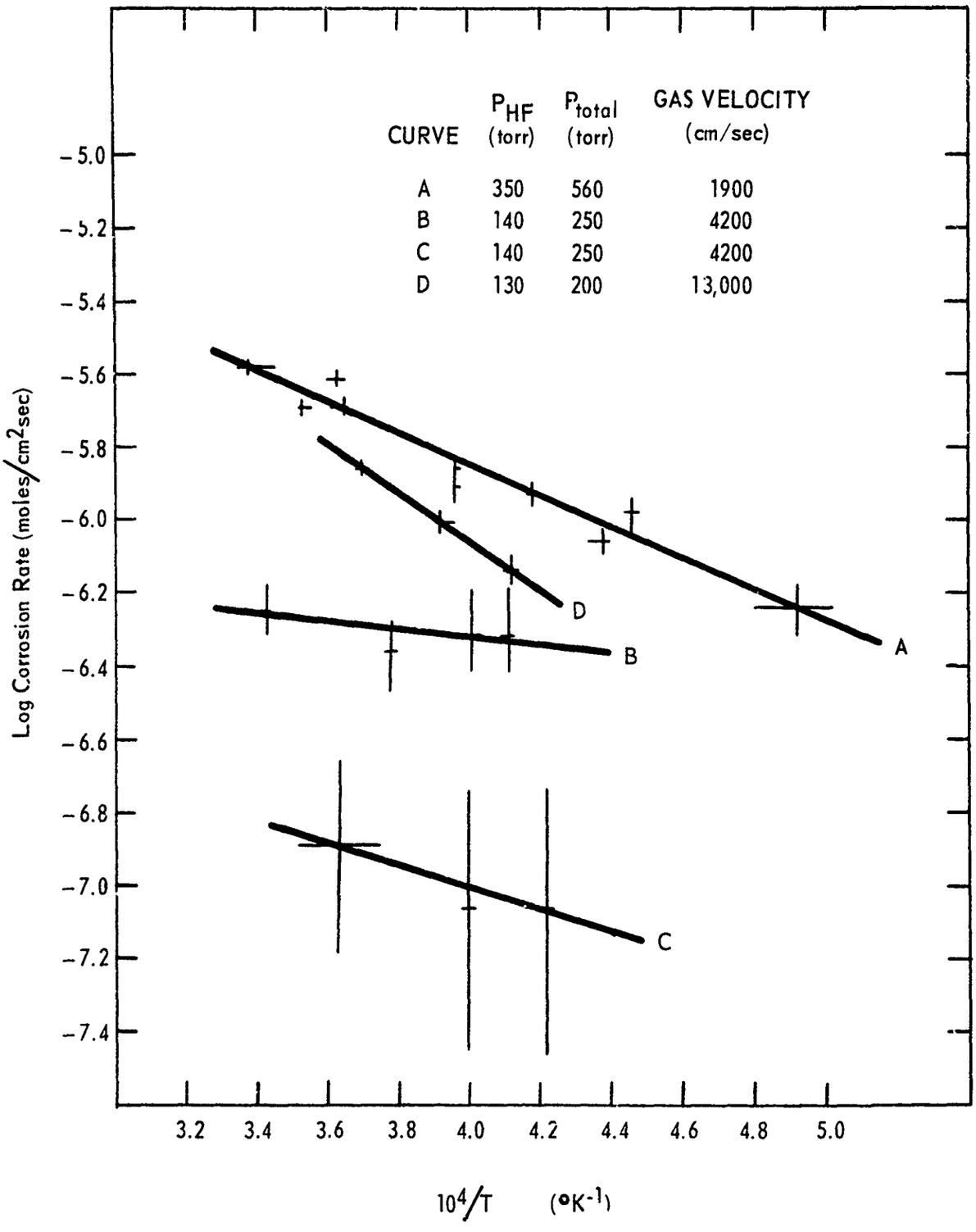

FIGURE A - 15 TEMPERATURE DEPENDENCE OF THE RATE OF REACTION OF W IN HF

4. Mass-Spectrometric Studies of Gas-Solid Reactions

P. O. Schissel
and O. C. Trulson

The objectives of the mass-spectrometric studies of gas-solid reactions are to identify reaction products and, from measurements of the temperature and pressure dependences of their rates of formation, to deduce the reaction mechanisms; these results are intended to be useful in analyses of kinetic data taken at higher pressures. As shown in Fig. A-16, the samples are resistively-heated ribbon filaments contained in a water-cooled chamber connected to the source chamber of a 60°-sector, Inghram-type mass spectrometer. Reactant gas at low pressure completely surrounds the sample. The reaction chamber is separated from the source chamber by an externally-operated shutter so that condensible product species emanating from the filament can be distinguished from background species of the same integral mass which normally occur in the vacuum system. Product species are ionized in the source by an electron beam; the ions are accelerated through an electrostatic lens, mass selected in the magnetic field, and preamplified by an electron multiplier detector, the output of which is displayed continuously on a strip-chart recorder. The output current is directly proportional to the rate of desorption of product species from the filament. Because of the high sensitivity of the detection system and the mass discrimination feature of the magnetic analyzer (resolution near 1/1000), desorption rates near 10^{12} molecules/cm^2 sec can be detected easily with this system.

The first experimental results were obtained for the oxygen-tungsten reaction,[1] where the products are condensible and reasonably abundant, and the solid surface remains free of oxide scale at the high temperature and low pressure conditions of the study. From the pressure and temperature dependences of the various species a kinetic model was proposed to explain the rates of formation of species in terms of the surface coverage of tungsten with oxygen. As a natural extension to this work, reactions of other oxidizing gases with tungsten are being studied. It seems reasonable to assume that once the oxygen is abstracted from such gases and adsorbed the various kinetic steps will proceed according to the model proposed for the oxygen-tungsten reaction; comparison experiments are indicated. During this report period the reactivity of tungsten with O_2 and CO_2 was compared.

The CO_2-W reaction is more complex than the O_2-W reaction since, in addition to O_2 and the tungsten-oxygen products, CO(g) is produced at a high rate at high temperatures. Furthermore, the rates of product formation are much lower with CO_2 than with O_2; this increases the experimental difficulty, particularly under low-pressure conditions.

Analysis of the mechanism for the O_2-W reaction was possible because the most important kinetic steps were the adsorption and desorption of oxygen, with the formation of product species only slightly perturbing a steady-state surface coverage by oxygen. The CO_2-W reaction appears to behave similarly. The rate of production of oxygen atoms from CO_2 is compared to that from O_2 in Fig. A-17 with the pressures of CO_2 and O_2 adjusted such that the molecular fluxes of CO_2 and O_2 striking the filament were approximately 2/1. At high temperatures the curves reach the same plateau, where earlier it was demonstrated that the plateau for oxygen corresponds to complete dissociation of the oxygen. Consequently it is assumed that at high temperatures the chief reaction between CO_2 and tungsten is merely dissociation of CO_2 to give CO and O(g). At lower temperatures the rate of formation of O(g) falls more rapidly when CO_2 is the source of oxygen, suggesting that the adsorption of oxygen from CO_2 is activated and becomes a rate-limiting step in the oxidation reactions.

Below 2500°K, O_2 is much more effective than CO_2 in producing WO_2(g) (Fig. A-18) while WO_3(g), an important product of the O_2-W reaction, is barely detectable with CO_2. At approximately 2700°K the rates of formation of WO_2 become asymptotically equal for the two oxidizers, while at higher temperatures the rate from O_2 begins to increase again while WO_2 from CO_2 continues to decrease. At present there is no conclusive explanation for the upturn in the WO_2 rate with O_2 as oxidizer.

In the earlier study[1] of the tungsten-oxygen reaction WO(g) was only qualitatively measured since the high mercury background from the diffusion pumps overlapped WO in the mass spectrum, making a shutterable WO

signal extremely difficult to obtain. The proposed kinetic model therefore did not account for WO. During this [illegible] period, the system was baked and pumped for several days to reduce the background until the WO could be observed. The rates of production of WO(g) using O_2 and CO_2 (Fig. A-19) are similar to those for O(g)(Fig. A-17); when CO_2 is substituted for O_2, the rate of formation of WO(g) at low temperatures is decreased, the fractional decrease being about the same as for O(g), while at high temperatures the rates with both gases are equal.

The results for O(g), WO_2(g), and WO(g) show that a new rate-limiting process is operative when CO_2 is the oxidizer. Two possibilities are immediately suggested: (1) CO(g), which is inevitably present, adsorbs on the surface and inhibits the oxidation; (2) the adsorption of oxygen onto tungsten from CO_2 is activated. The first possibility is unlikely because when the rate of formation of tungsten oxides was observed first with only O_2 present, then with approximately ten times as much CO as O_2, no change in the rate of oxidation was observed. The simplest way to approach the second possibility is to assume that CO_2 as an oxidizer merely has extra difficulty in delivering oxygen to the surface but that once this is accomplished all the surface and desorption reactions are the same as with O_2 as oxidizer. A consequence of this assumption is that, when CO_2 is substituted for O_2, the fractional decrease in WO_2(g) production at low temperatures should be the square of that in O(g) production, since the latter is proportional to the first power of the fractional surface coverage by adsorbed oxygen and the former to its square.* For example, the rate of formation of O(g) at ~2000°K is given by[1]

$$r_3 = k_3\theta_2 \simeq \frac{k_3}{k_2^{1/2}} (s\nu P)^{1/2}$$

where s, the sticking coefficient, has been taken as 1 for oxygen. At 2000°K with CO_2 as oxidizer near 10^{-4} torr pressure, r_3 is approximately 1/6 that when O_2 is used; therefore, $s \simeq 1/36$ at this temperature and pressure so that the ratio of WO_2 intensities with CO_2 and O_2 should be near 1:36. The data

---

* That WO(g) decreases similarly to O(g) would be expected if only one surface oxygen atom were involved in both cases. The significance of this cannot be assessed until the place of WO(g) in the model is better understood.

in Fig. A-18 correspond very nearly to this ratio. However, the model would also predict that WO_2 and WO_3 production rates would decrease by the same fraction, seemingly in contradiction to the WO_3 results obtained with CO_2, though these are not conclusive.

The relative reactivities of O(g) and CO_2(g) were studied using the two filament system shown in Fig. A-20. The reaction of CO_2 with tungsten to form WO_2 was observed directly from the first (sample) filament at several temperatures. At each temperature the second (source) filament was turned on momentarily to a temperature sufficient to crack every CO_2 striking the tungsten to CO + O(g); a fraction of this O(g) then struck the sample filament and reacted to form additional WO_2. On turning on the source filament, the rate of formation of WO_2 increased much more at low sample filament temperatures than at high (Fig. A-21). These results are in accord with the results of the W-O_2 and W-CO_2 reaction comparison and emphasize the comparable reactivity of tungsten with atomic and molecular oxygen.

Future Work

It is planned to continue the oxygen studies with the substrates Ir, C, and carbides and to initiate measurements using H_2O as oxidizer with a tungsten substrate.

References

1. P. O. Schissel and O.C. Trulson, "Mass Spectrometric Study of the Oxidation of Tungsten," Technical Report No. C-26, Contract DA-30-069-ORD-2787, October 1964.

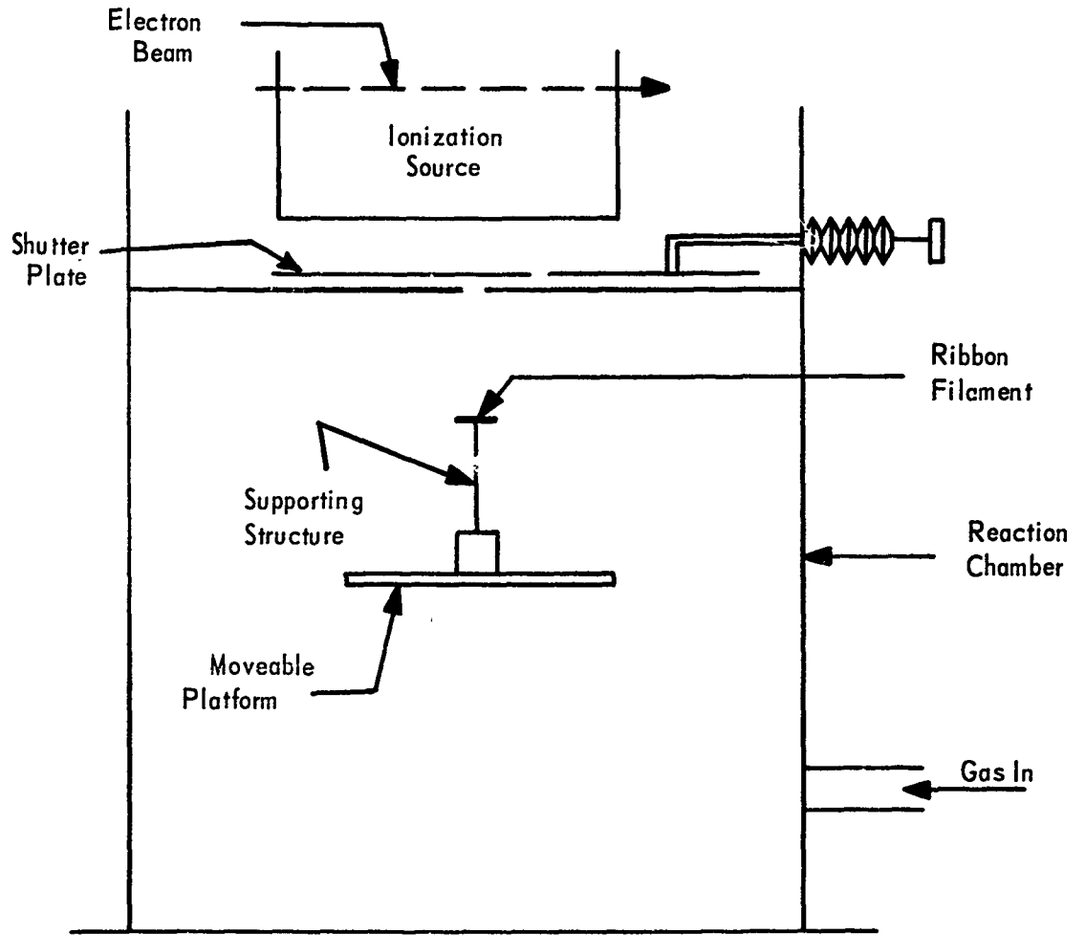

FIGURE A - 16 SCHEMATIC VIEW OF APPARATUS USED FOR REACTION MEASUREMENTS.

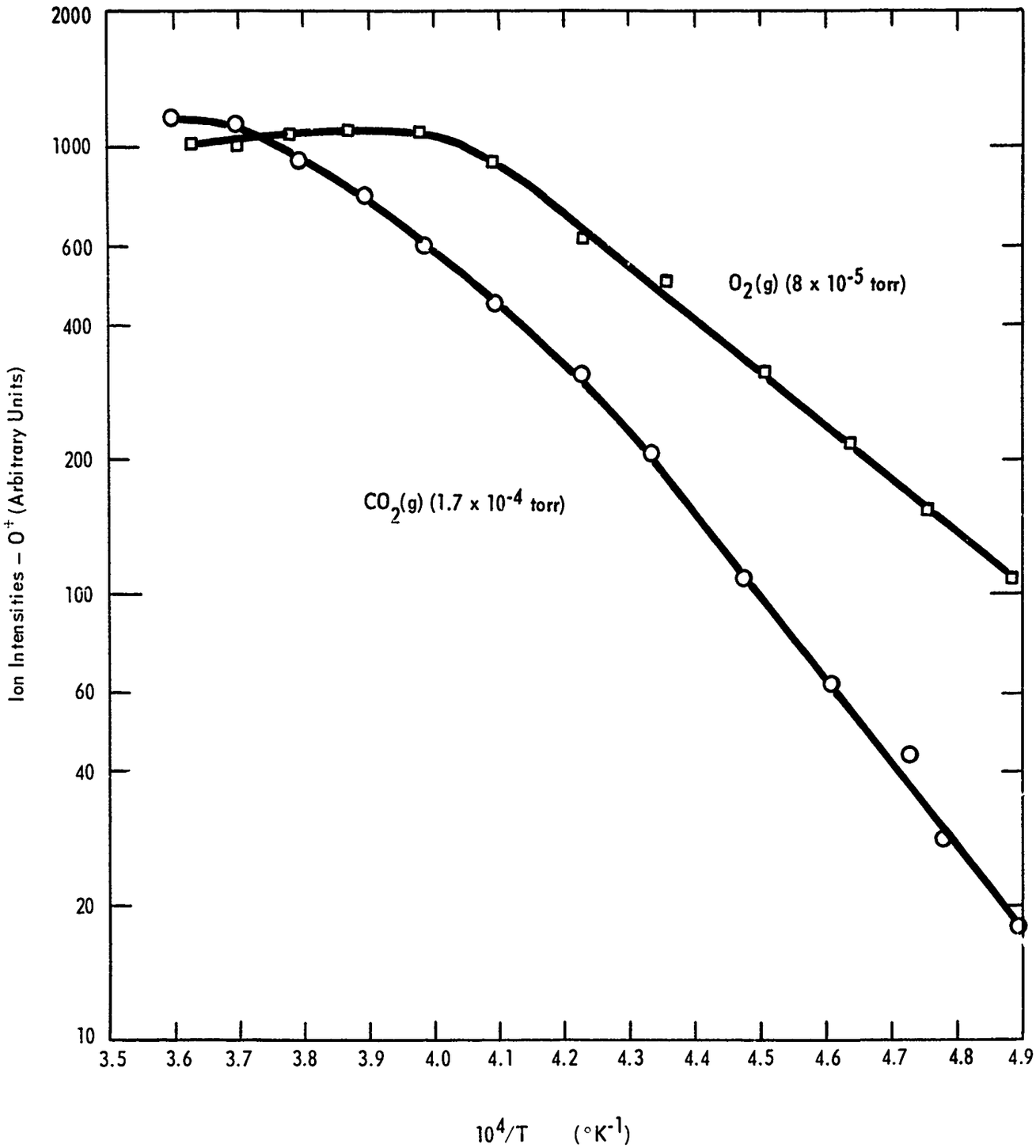

FIGURE A - 17 RATE OF PRODUCTION OF O(g) FROM REACTION OF O_2 AND CO_2 WITH W

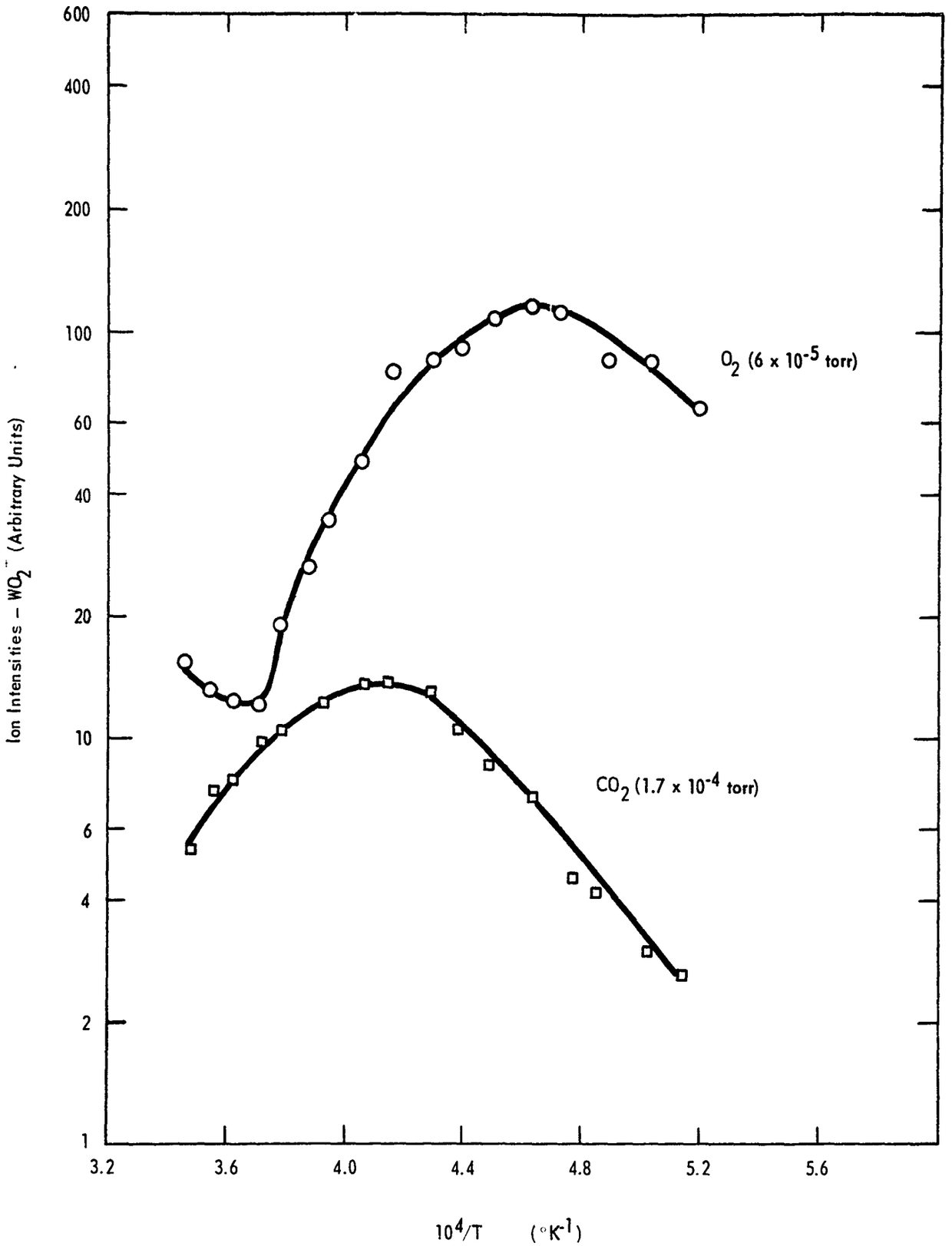

FIGURE A - 18 RATE OF PRODUCTION OF WO_2(g) FROM REACTION OF O_2 AND CO_2 WITH W

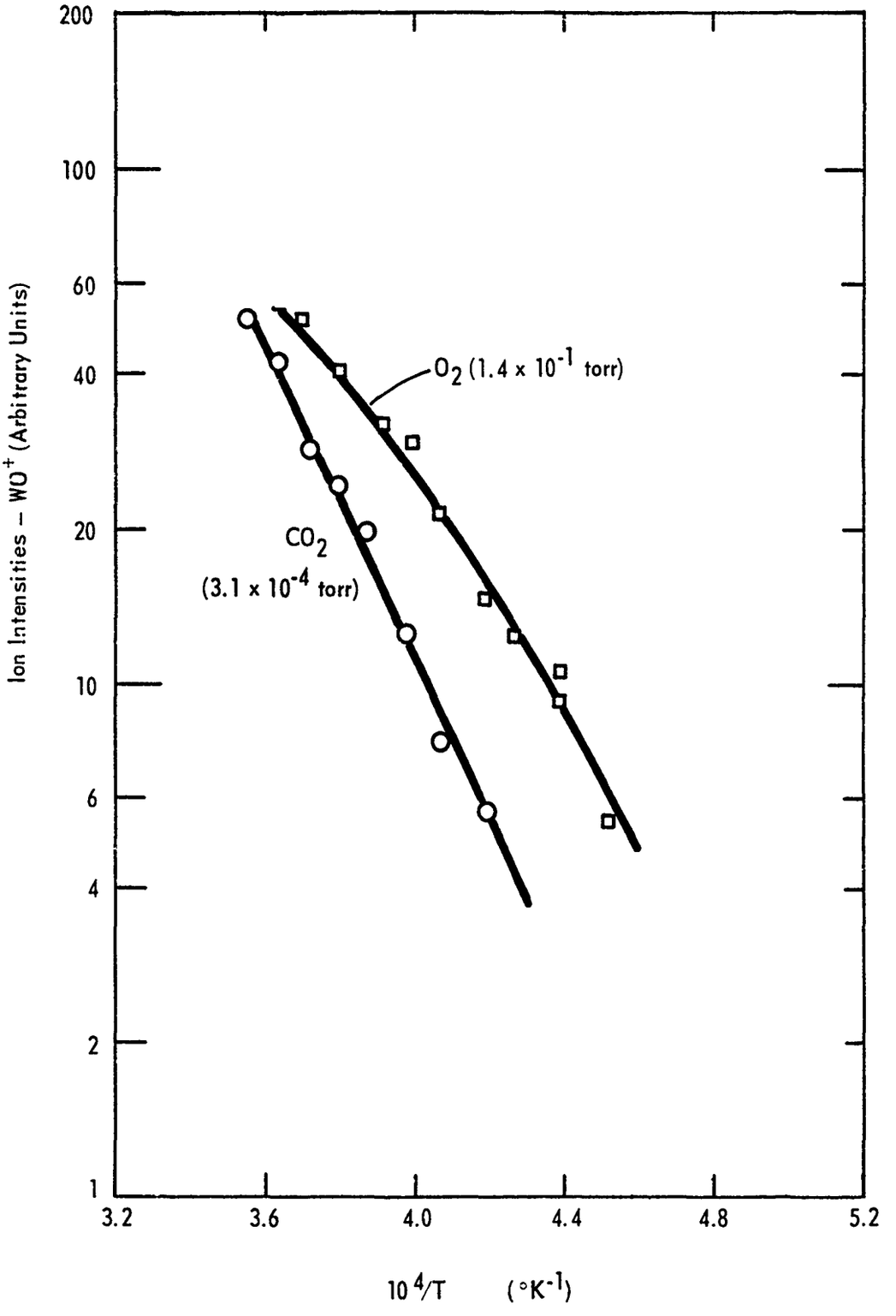

FIGURE A - 19 RATE OF PRODUCTION OF WO(g) FROM REACTION OF O AND CO WITH W

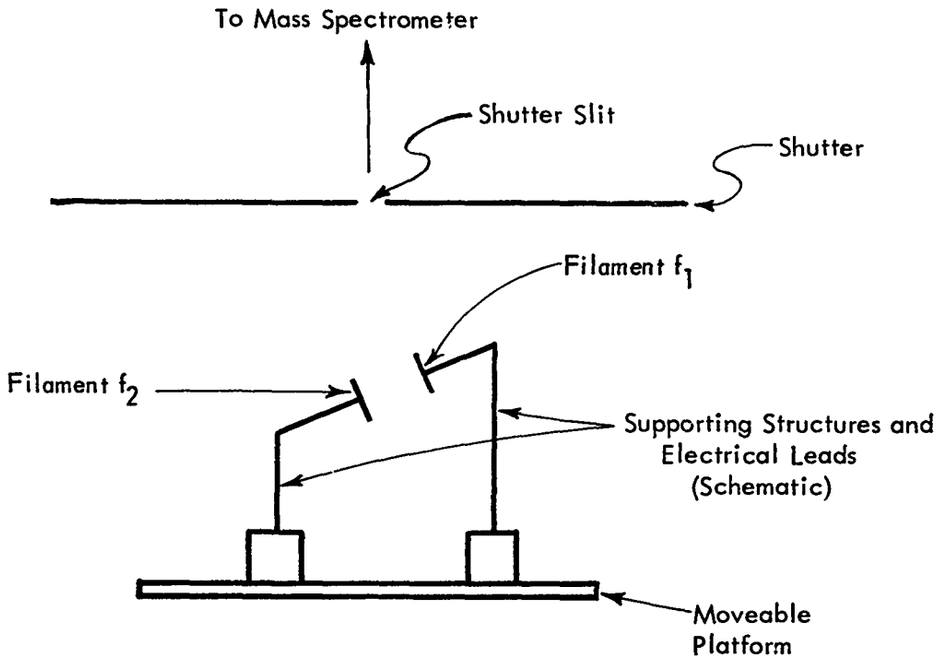

FIGURE A - 20 SCHEMATIC VIEW OF APPARATUS USED FOR REACTION OF ATOMIC OXYGEN AND TUNGSTEN

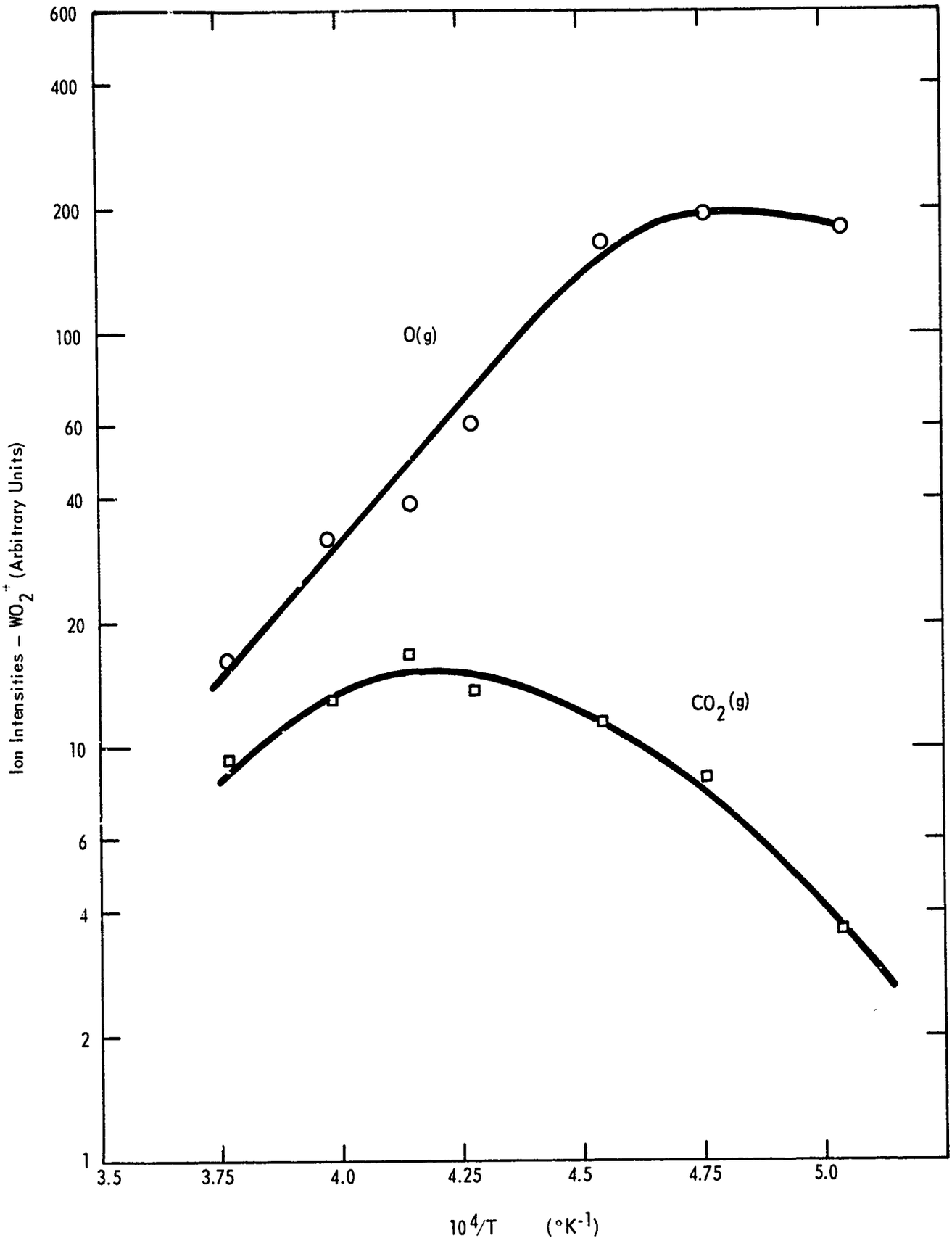

FIGURE A - 21 RATE OF PRODUCTION OF WO_2(g) FROM REACTION OF O(g) AND CO_2(g) WITH W.

5. Rocket-Nozzle-Insert Test and Analysis Program

An essential phase of this program is to put our derived rate equations to the test of predicting corrosion rates in small liquid motor firings. The firings are to be carried out in such a way that the partial pressures of the species in the exhaust and the temperature of the insert (as a function of time) can be determined or reliably calculated. Using this information and reaction rate data developed in the laboratory the nozzle-insert corrosion will be predicted and compared with experimentally measured corrosion. Computer programs for this purpose are partially completed but await final clarification of the kinetics of the important reactions.

The firings, to be carried out by the Propulsion Laboratory, Directorate of Research and Development, Army Missile Command, Redstone Arsenal, are to be done with a liquid fuel motor since it operates reproducibly and the concentrations of exhaust species can be varied within limits by changing the propellant mixture. The test motor (UDMH-IFRNA) is to operate with constant fuel and oxidizer feed rates at chamber pressures up to 1000 psi. Pressure as a function of time is to be determined to ± 1/2% at 1000 psi.

The nozzle inserts are to be furnished by UCRI mounted in stainless steel aft closures designed to bolt on the AMC motor. Determination of insert interior surface temperature is a major experimental problem. The initial inserts will be furnished with thermocouples for temperature measurement.

Two 0.5 inch i.d. tungsten inserts, thermally insulated from their stainless steel holders by PC-60 graphite and pyrolytic graphite have been completed; the one shown in Fig. A-22 is instrumented with three probe type thermocouples located at varying radial depths, the other with one tungsten Nanmac surface-type thermocouple. In addition, three ATJ graphite inserts and holders were constructed and sent to the Propulsion Laboratory. These are to be used for checking our nozzle design and for initial trials of the test motor.

The new test motor procured by the Propulsion Laboratory malfunctioned during initial firings and has to be rebuilt, so tests of holder design and thermocouple instrumentation could not be made this quarter.

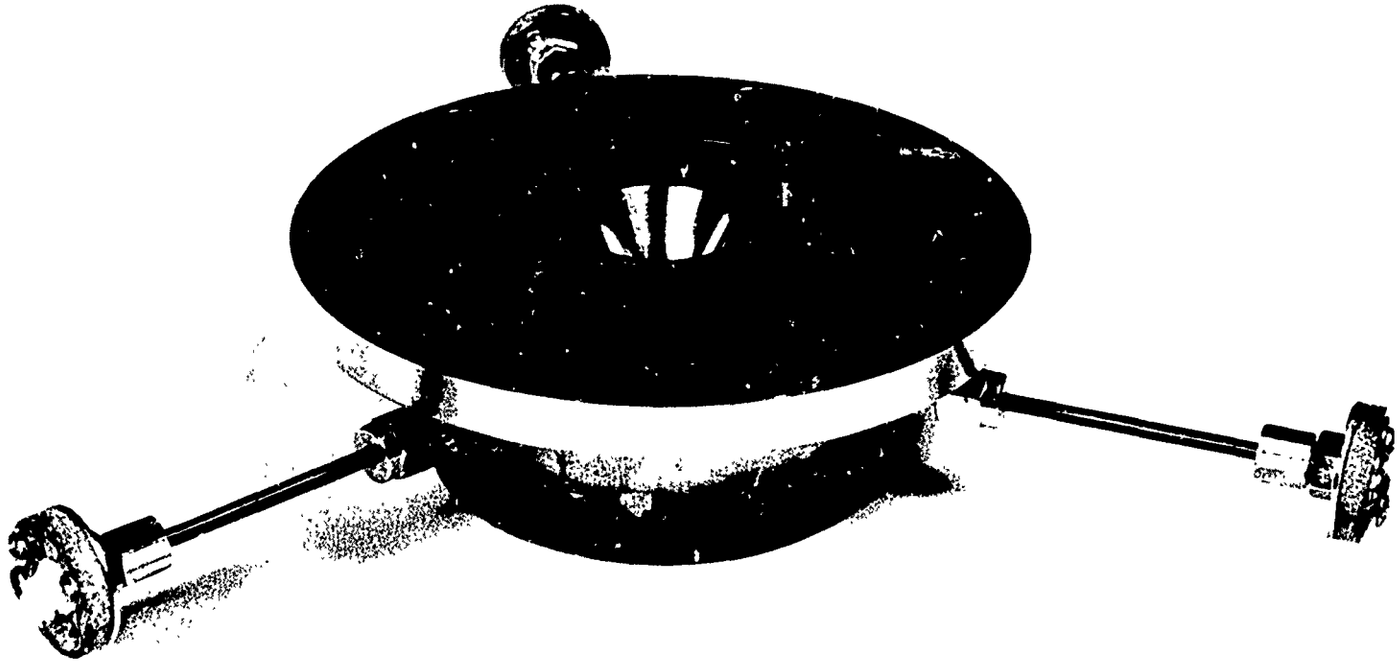

FIGURE A - 22 TUNGSTEN INSERT AND HOLDER

B. Skeletal Carbide Composites

1. Introduction

The need for high temperature nozzle inserts compatible with the propellant exhausts has focused interest on the very high melting point materials: refractory metals and their alloys, oxides, carbides, borides, nitrides, zirconates, silicates, silicides, and mixed ceramic bodies. As a group. the refractory carbides, NbC (6330°F), TaC (7010°F), ZrC (6107°F), and HfC (7030°F) have the highest known melting points and have good strength and creep resistance at high temperatures. However, when compared to metals, they are more brittle at low temperatures and are more susceptible to thermal shock failure. Composites containing both refractory carbides and metal phases are therefore required to exploit the desirable properties of the refractory carbides.

The distribution of the metal phase is an important factor affecting the performance of the composite. The possible distributions of the phases are: continuous metal, discontinuous non-metal phases; two interlocking continuous phases; continuous non-metal, discontinuous metal phases. Studies on continuous metal – discontinuous non-metal phase systems have led to a number of useful composite materials. Excellent practical examples are the cobalt-bonded refractory carbides, SAP (sintered aluminum powder), and TD (thoria dispersed) nickel. However, the melting points of the metals limit the maximum temperature at which these can be used. Composites with two interlocking continuous phases avoid this limitation and the configuration is promising for materials with good room-temperature strength, acceptable thermal and mechanical shock resistance, and good high-temperature strength and creep behavior. In many cases the lifetime required of such material is of the order of minutes and there is no thermal cycling, i.e., there is only a heating cycle. A successful example has been the two-phase composite of silver and tungsten that is being used in some uncooled solid-fuel rocket-nozzle throats. This material is impressive, since it is one of the few composites which manages to combine most of the desirable properties of both component phases while minimizing the undesirable qualities of each. Other work on silver-infiltrated porous alumina bodies has

not been as successful because of bonding problems and interior cracking of the non-metal skeleton, probably because of thermal-expansion mismatch between the two phases.[1]

The refractory-metal carbides are attractive as one component of a system consisting of two interlocking continuous phases because of their high melting points, strength at high temperatures, and the ease with which they are wetted or bonded by many molten metals. The introduction of a continuous metal phase into a carbide material can increase the thermal conductivity and the tensile and impact strengths of the material. Thus, when the material is being subjected to thermal shock, higher conductivity would mean lower temperature gradients, hence lower thermal stresses, and the higher tensile strengths would provide greater resistance to these stresses. By properly selecting the composite structure it should be possible to greatly improve the room-temperature impact strengths of metal-ceramics while retaining their desired high-temperature strengths.

In our studies, emphasis is placed on <u>interlocking</u> systems of two continuous phases where one phase is a refractory-metal carbide and the other a metal or alloy.

2. Preparation — I. Binder

The skeletal carbide composites for our studies were made by reacting carbon or metal powders to refractory carbide powders, consolidating these powders to form strong self-bonded porous bodies and then infiltrating with metal.

<u>Powders</u> - The powders for making the self-bonded bodies were prepared by direct reaction of high purity metal hydride or metal powders and spectroscopic grade carbon. The powders were intimately mixed and lightly pressed into blocks (using a small amount of camphor as a fugitive binder and lubricant). These were then placed on a refractory carbide platform in a graphite crucible and heated in a flowing H_2 atmosphere. The reacted blocks, which were quite friable, were broken into powders in a crushing mortar. The powders were then screened and the minus 270 mesh fraction used for preparing the carbide bodies. The particle size of the fraction used, as measured with a Fisher Sub-Sieve Sizer, is usually about seven microns.

In some cases the powders were further purified by heating in a vacuum furnace for extended periods of time. TaC powders prepared in this way were nearly stoichiometric in composition and of excellent purity as shown by chemical analysis.

TABLE B-I - ANALYSES OF UCRI TaC*

Lot	Ta	C_{Total}	C_{Free}	$C_{Combined}$	Ta + C_C	Atom Ratio C_C/Ta
C-242B	93.82	6.19	0.07	6.12	99.94	0.985
C-227B	93.81	6.18	0.06	6.12	99.93	0.985
C-252B	93.87	6.27	0.03	6.24	100.11	1.00

	Spectrcchem. Trace Anal. Total	N	O	Total Impur.	Total Anal.
C-242B	0.0055	0.01	76 ppm	0.09	100.03
C-227B	0.0057	0.01	90 ppm	0.135	100.065
C-252B	0.0051	< 0.01	94 ppm	0.04	100.15

* Analysis in weight percent except as noted.

High purity powder batches of TaC, ZrC, 90 TaC/10 ZrC, 80 TaC/20 ZrC, 90 TaC/10 HfC, and 80 TaC/20 HfC were produced. The principal effort was on preparing twenty-five pounds of TaC to be used for isostatic pressing studies.

Consolidation of Refractory Carbides - The powders, loaded and leveled into closed graphite dies, were hot pressed to form strong self-bonded bodies. The dies were heated in air to a maximum external temperature of 5200°F and pressures of 5000-7000 psi applied. The entire pressing cycle required about five minutes. No significant reaction of the pressed carbide bar with the die occurred. The density of the self-bonded piece depends upon particle size and upon the pressure, temperature and time at temperature during the heating cycle.

The refractory carbide skeletons used were usually pressed to a density of 80%-85% of the theoretical density of the carbide. Electrical resistivity measurements, used for quality control, detect the presence of internal cracks or other irregularities. The self-bonded carbide bodies produced in this manner were used either to study the behavior of self-bonded material or for infiltration by a continuous metal phase.

Isostatic pressing with subsequent sintering was used to produce larger specimens than are possible with our hot-pressing equipment. Our isostatic press has a working chamber of 3 in. i.d. by 18 in. long and working pressures up to 60,000 psi. Room temperature isostatic pressing produces uniform, comparatively low density (55-60% theoretical density) TaC bodies requiring further sintering to produce a strong carbide skeleton for infiltration. With such low initial densities it has not been possible to sinter the pressed material to a sufficiently strong body. With 1 wt % cobalt added to the starting TaC powder as a sintering aid — and subsequently vaporized — a strong carbide body (0.7 in. diameter and about 70% theoretical density) was produced and successfully infiltrated with 90 Ag/10 Cu alloy. Properties of this material are not yet available. All materials reported were produced by hot-pressing techniques.

Infiltration - The metal infiltrant must: (1) form a strong bond with the carbide grains, (2) largely fill the pores of the TaC skeleton, and (3) not cause a disruption or weakening of the bonds between the carbide grains, either during infiltration or during vaporization at operating temperatures. For the composites reported here, the metal or metal alloy was infiltrated by placing it on top of the self-bonded carbide piece and heating in an argon atmosphere. Upon melting, the metal infiltrates the carbide body. After infiltration, the density of the piece is determined and its soundness checked by resistivity measurements. From measurements of the densities of the composites so far prepared, we have found that more than 2/3 of the porosity of the self-bonded carbide body is filled with metal.

Silver, copper, and silver-copper alloys are successful infiltrants while nickel, cobalt, nichrome, and platinum infiltrate satis-

factorily but disrupt the carbide grain-to-grain bonds either while they are being introduced or upon being heated to temperatures above the melting point of the metal. A rapid test to determine whether the infiltration of the metallic phase has damaged the continuous carbide skeleton is to evaporate the metal phase from the infiltrated piece in a vacuum or non-oxidizing atmosphere. If the materials chosen and the fabrication techniques are suitable the carbide skeleton remaining will be essentially unchanged from the initial self-bonded skeleton. Our TaC-Ag composites subjected to this test do not show changes in density, electrical resistivity, or transverse rupture strength of the carbide skeletons.

3. Physical and Mechanical Properties — I. Binder, R. W. Kebler

Nickel-Infiltrated Carbides - The room-temperature transverse rupture strength of the TaC-Ni composite was nearly four times that of self-bonded TaC but its strength was not maintained at temperatures approaching the melting point of nickel (Fig. B-1). Evidently the nickel partially dissolved and partially destroyed the carbide-to-carbide grains. Attempts were made to "presaturate" the nickel by heating it in contact with TaC to 1475°C before infiltration. This did not work as TaC infiltrated with "presaturated" nickel also did not maintain its strength at temperatures above 1300°C. Similar behavior was observed for cobalt-infiltrated TaC and nickel-infiltrated ZrC.

No further work is to be done with nickel or cobalt as an infiltrant for skeletal carbides.

Silver and Silver Alloy Infiltrated Carbides - Further transverse rupture strength data confirmed the desired behavior of the TaC-Ag composite (Fig. B-1) reported in the December, 1964, Quarterly Progress Report, Contract DA-30-069-ORD-2787. The room-temperature strength (78,000 psi) is nearly double that of the self-bonded carbide and the TRS is comparable to that on the self-bonded carbides at high temperatures.

Improved lower temperature strengths were sought by alloying the silver to obtain improved wetting of the TaC and/or strengthening of the metal phase. Two silver-copper alloys were used to infiltrate TaC bodies.

In both cases the TRS (Tables B-II and B-III) was comparable at room tem-

TABLE B-II TRANSVERSE RUPTURE STRENGTH

TaC - 9 wt.% (90 Ag/10 Cu)

Temperature (°C)	TRS (lbs/in^2)
RT	74,000
1100	20,000
1320	21,000
1485	22,000
1700	23,000
1940	59,000

TABLE B-III TRANSVERSE RUPTURE STRENGTH

TaC - 9.8 wt.% (50 Ag/50 Cu)

Temperature (°C)	TRS (lbs/in^2)
RT	81,700
940	15,200
1070	15,800
1470	15,650
1815	16,100

perature to that found for TaC-9 wt % Ag and was consistently lower in the temperature range 900-1800°C. In the simple copper-silver alloys the high-temperature strength is maintained, but as infiltrant metal for skeletal carbide composites they do not lead to better mechanical properties than found for silver alone.

The addition of small amounts of nickel or cobalt to silver should give an infiltrant with better wetting properties. This alloy infiltrates TaC readily and gives higher room-temperature TRS. However, even this small amount of nickel apparently leads to disruption of the carbide-to-carbide grain boundaries and so to loss of strength as the melting point of the metal alloy is approached, (Table B-IV).

TABLE B-IV TRANSVERSE RUPTURE STRENGTH

TaC + 10 wt % (98 Ag/2 Ni)

Temperature (°C)	TRS (psi)
RT	94,000
840	34,000
945	20,000
1080	4,000

Similar behavior was found for both a TaC-10% (98 Ag/2 Co) composite and a ZrC-10% (98 Ag/2 Ni) composite.

80 TaC/20 ZrC and 80 TaC/20 HfC Bodies - Certain alloys of IV and V group metal carbides have melting points as high or higher than TaC. In addition the products formed upon oxidation are higher melting than those from TaC and so may lead to improved resistance to corrosion. The transverse rupture strength of hot-pressed bars of 80 TaC/20 ZrC and 80 TaC/20 HfC was determined (Tables B-V and B-VI).

TABLE B-V TRANSVERSE RUPTURE STRENGTH

80 TaC/20 ZrC

Temperature (°C)	TRS (psi)	% Theoretical Density
RT	45,000	79
1104	23,800	74
1394	21,200	71
1630	22,700	72
1820	16,500	70
1995	32,400	74

TABLE B-VI TRANSVERSE RUPTURE STRENGTH

80 TaC/20 HfC

Temperature (°C)	TRS (psi)	% Theoretical Density
RT	27,600	72
870	19,200	71
1150	20,200	71
1380	20,700	71
1635	23,000	-
1905	28,600	73
1970	24,600	75

The strengths are less than found for TaC but the porosity of the carbide alloys is significantly higher. An interesting feature is the small variation in strength with temperature (for equal density specimens). The results are encouraging and further studies, especially of oxidization resistance, will be made.

4. Vaporization and Corrosion — I. Ladd, R. W. Kebler

Rates of heating, vaporization of silver, and chemical corrosion of a TaC-Ag and a commercial W-Ag composite were studied using an arc-image heated stagnation-point-flow reactor.

Melting and vaporization of Ag should reduce the rate of temperature rise, at constant heat input, for a small composite body as compared to the non-vaporizing part alone (TaC or W). Small specimens (1/4" x 1/4" x 0.1") were heated with constant radiant energy input and the temperature rise monitored. The temperatures given are brightness temperatures with constant emittance corrections of 0.5 for the porous TaC and TaC-Ag composites and 0.6 for the low density porous tungsten and W-Ag composites. Both the TaC-Ag and W-Ag composites definitely have lower rates of temperature rise than the uninfiltrated base materials (Figs. B-2 and B-3). For the sample sizes used here the cooling effect of the melting and vaporizing of the silver was not appreciable after about thirty seconds. This is consistent with measurements by weight loss of the rate of silver evaporated from TaC-Ag (Fig. B-4) showing that 90% of the silver is evaporated in abou thirty seconds.

The decreased rate of temperature rise for a given input of energy for the infiltrated TaC composite, as has been found for infiltrated tungsten composites,[2,3] is of major importance in increasing thermal shock resistance. This is a significant advantage of self-cooling composites of this type. The relative thermal shock behavior of self-bonded TaC and the TaC-Ag composite were compared using the arc-image source to rapidly heat one side of small rectangular bars. For the same radiation input the self-bonded TaC bar cracked in the first five seconds of heating while the TaC-8% Ag bars could not be cracked. Larger pieces of the composites are needed before complete thermal shock measurements can be made.

The chemical corrosion rates (Figs. B-5 and B-6) for the composites were obtained by heating them for specified periods in an argon-CO_2 gas stream. The temperatures (an emittance correction has been applied to the brightness temperature) given are the highest the specimens reached. Emittance for the TaC was taken to be 0.5, for the dense tungsten 0.42 to 0.43, and for the tungsten-silver composite 0.6. The linear recession rate, which is averaged over the heating period, was measured for two different time intervals. Within experimental error, the average linear corrosion rate was found to be the same for both time periods. The linear corrosion rate of the TaC-8% Ag composite as a function of temperature was found to be the same as for the TaC (83% dense) base material (Fig. B-5). These linear corrosion rates are comparable to those found in our earlier work for fully dense tungsten.

Similarly, linear corrosion rates of the W-9.5% Ag composite and the porous tungsten base material, prepared by vaporizing the silver from the composite in an inert atmosphere, were compared. The corrosion rates as a function of temperature, for both this low density, desilvered tungsten and the W-9.5% Ag composite, were the same within experimental error, but were several times greater than for fully dense tungsten (Fig. B-6). Although it is not clear why the W-Ag composite has such high linear corrosion rates compared to those of dense tungsten, it is obvious that the porous structure remaining after evaporation of the silver has a much increased surface area available for reaction. Furthermore, this large surface area is retained during reaction due to the immediate vaporization of tungsten oxide as it forms.

5. Future Program

Emphasis is to be placed on producing, using isostatic pressing, 1-1/2 inch diameter TaC-Ag specimens from which nozzle inserts can be made. These inserts will be tested for thermal shock and corrosion, relative to tungsten, in the AMC test motor.

Further studies on silver and copper as infiltrants are to be made. The influence on infiltration behavior and strength of small amounts of additives, such as molybdenum, to the copper and silver alloys are to be determined. The oxidation behavior of the TaC/ZrC and TaC/HfC alloys relative to that of TaC is to be evaluated.

References

1. T. H. Blakely and A. E. S. White, Plansee Proceedings, 1955, p. 335.

2. A. V. Levy, "Composite Materials for Solid Rocket Nozzles" (U) Bull. Interagency, Solid Propulsion Meeting, III, 397, (1963).

3. F. B. Gessner, J. D. Seader, R. J. Ingram, T. A. Coultas, J. Spacecraft and Rockets 1, 643 (1964).

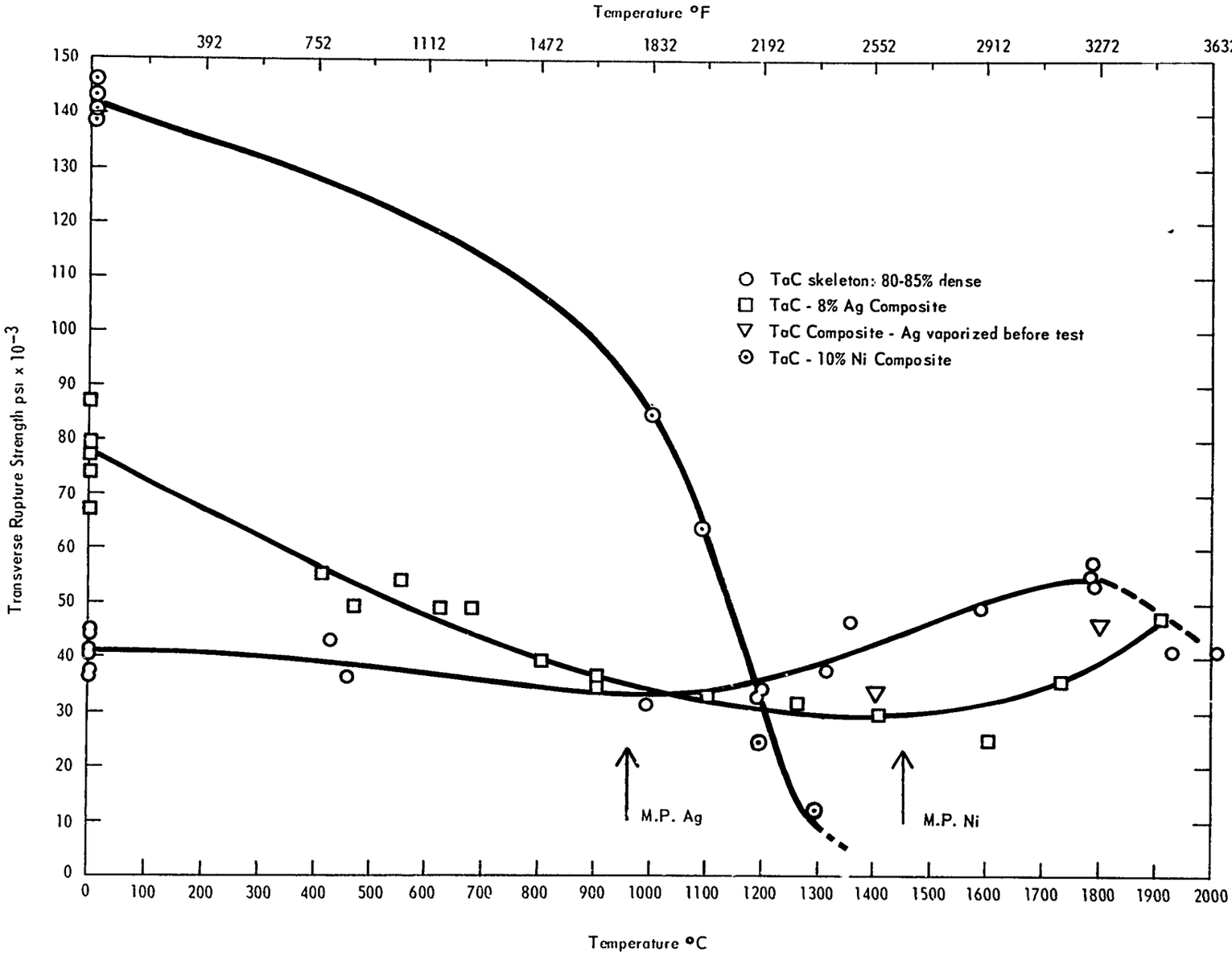

FIGURE B - 1 TRANSVERSE RUPTURE STRENGTH

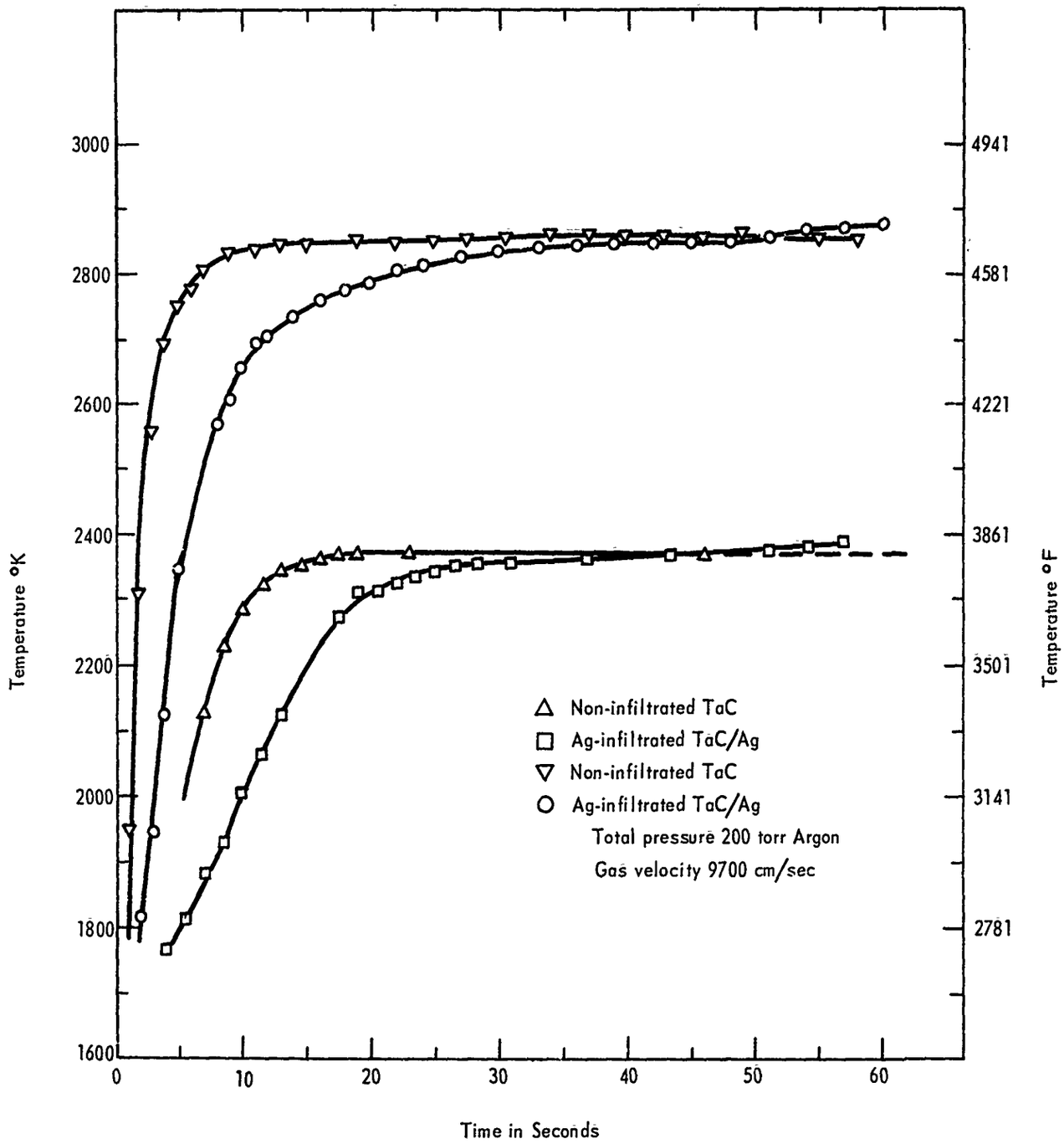

FIGURE B - 2 TIME-TEMPERATURE DEPENDENCE OF INFILTRATED AND NON-INFILTRATED TaC

The surface temperatures of the samples are plotted as functions of the time of exposure in an arc-image furnace.

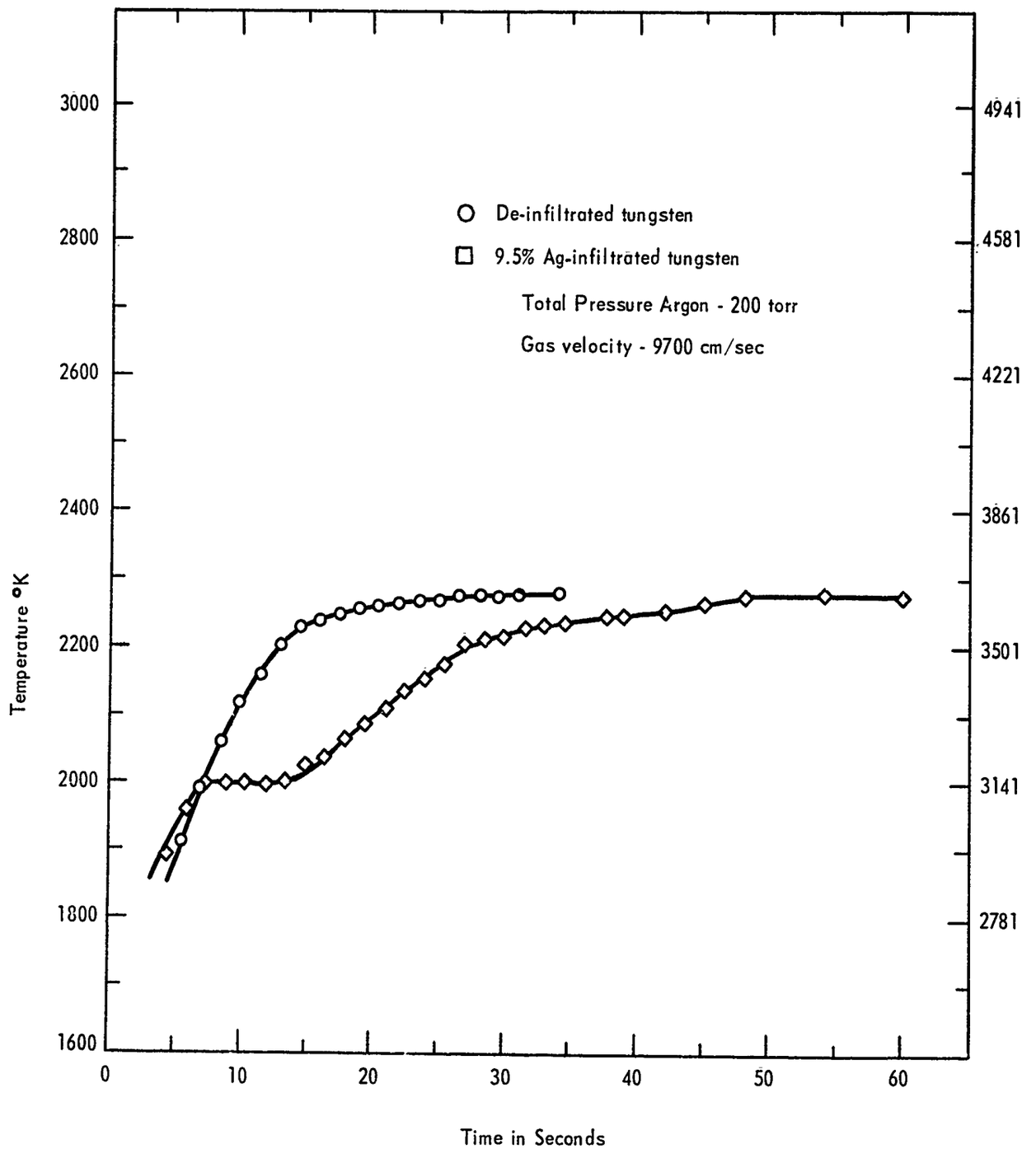

FIGURE B - 3 TIME-TEMPERATURE DEPENDENCE OF INFILTRATED AND DE-INFILTRATED TUNGSTEN

The surface temperatures of the samples are plotted as functions of the time of exposure in an arc-image furnace.

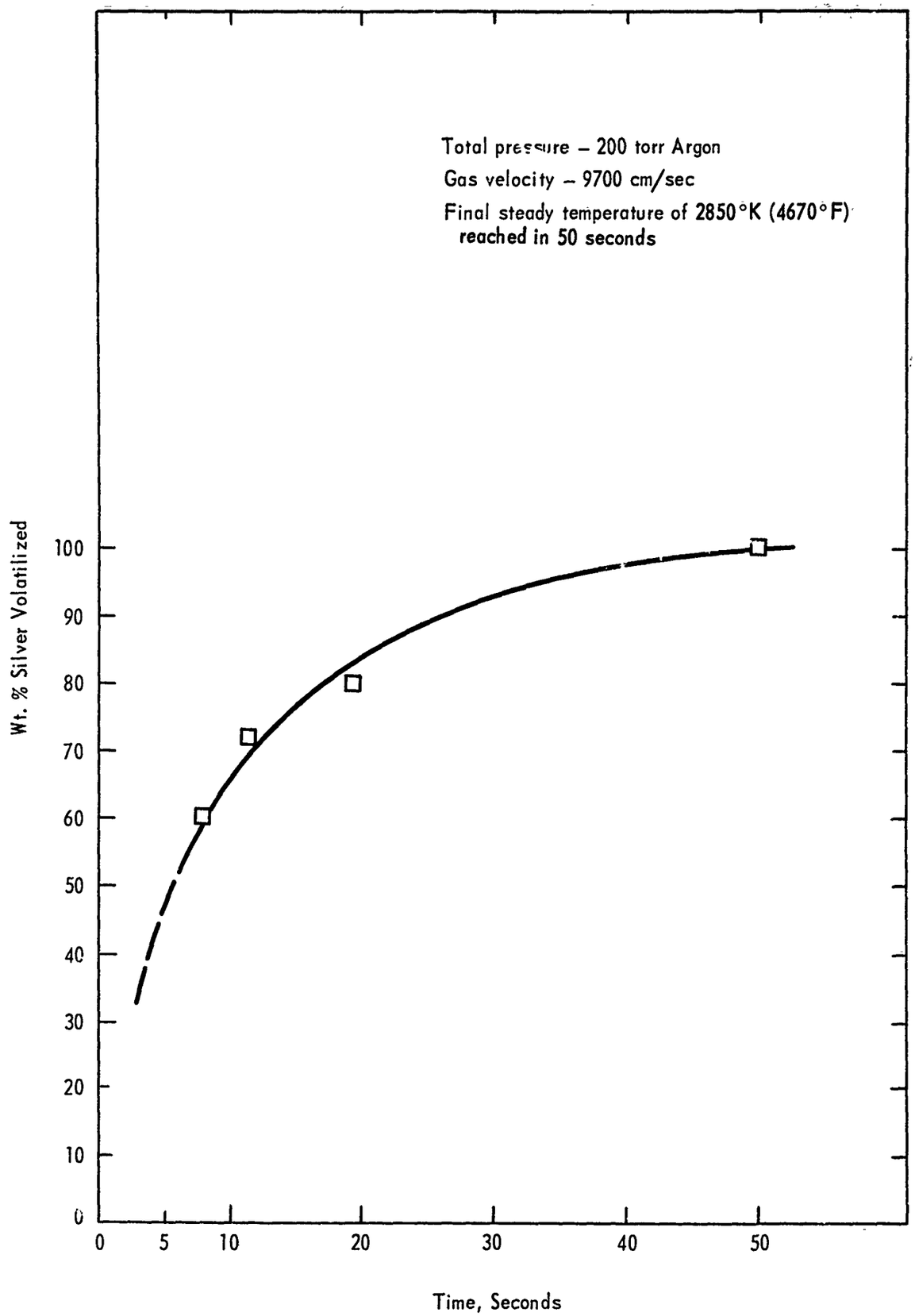

FIGURE B - 4 LOSS OF SILVER FROM TaC-Ag COMPOSITE WITH TIME

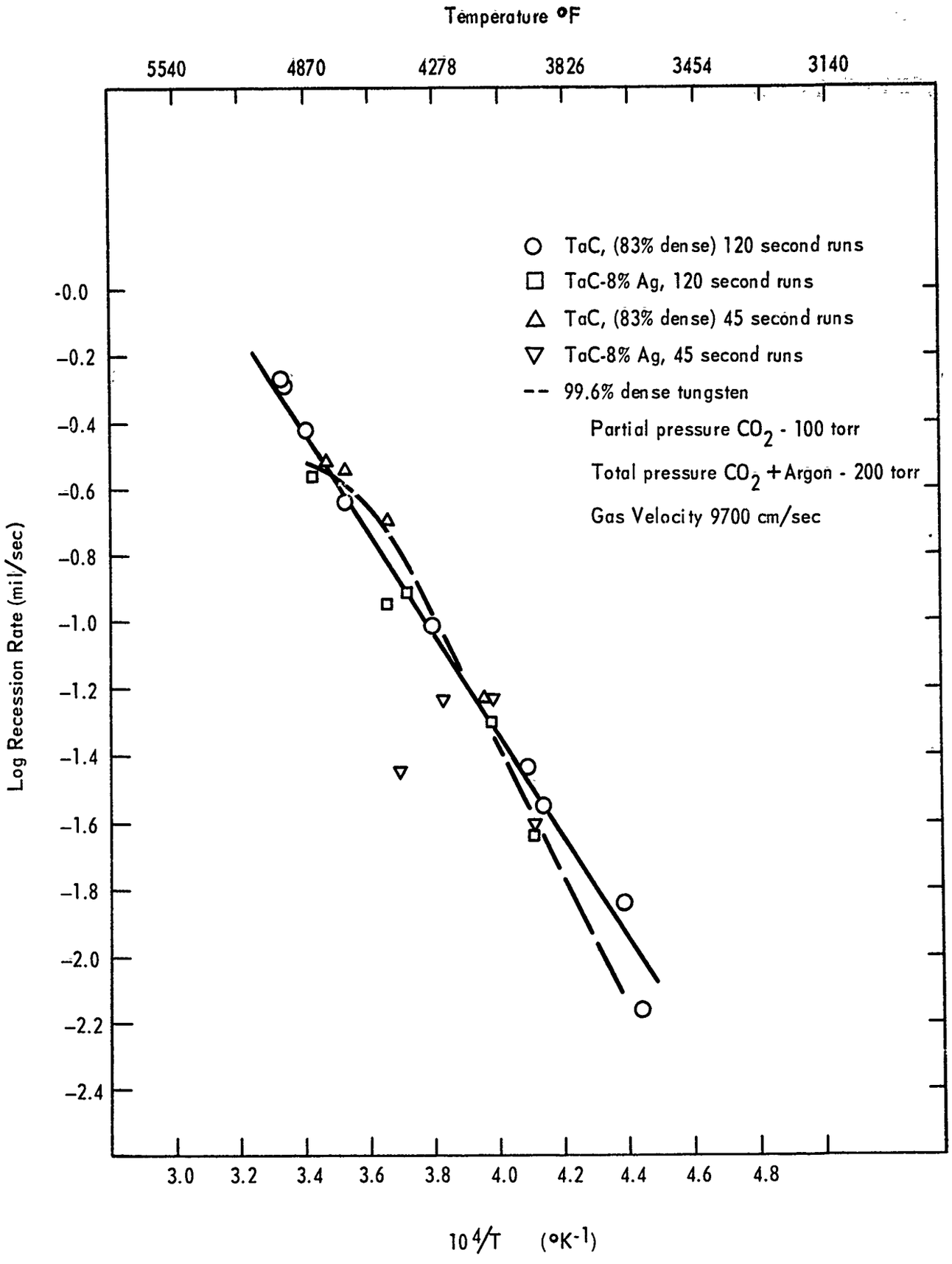

FIGURE B - 5 TEMPERATURE DEPENDENCE OF THE RECESSION RATE OF HOT-PRESSED TaC AND TaC/Ag IN CO_2

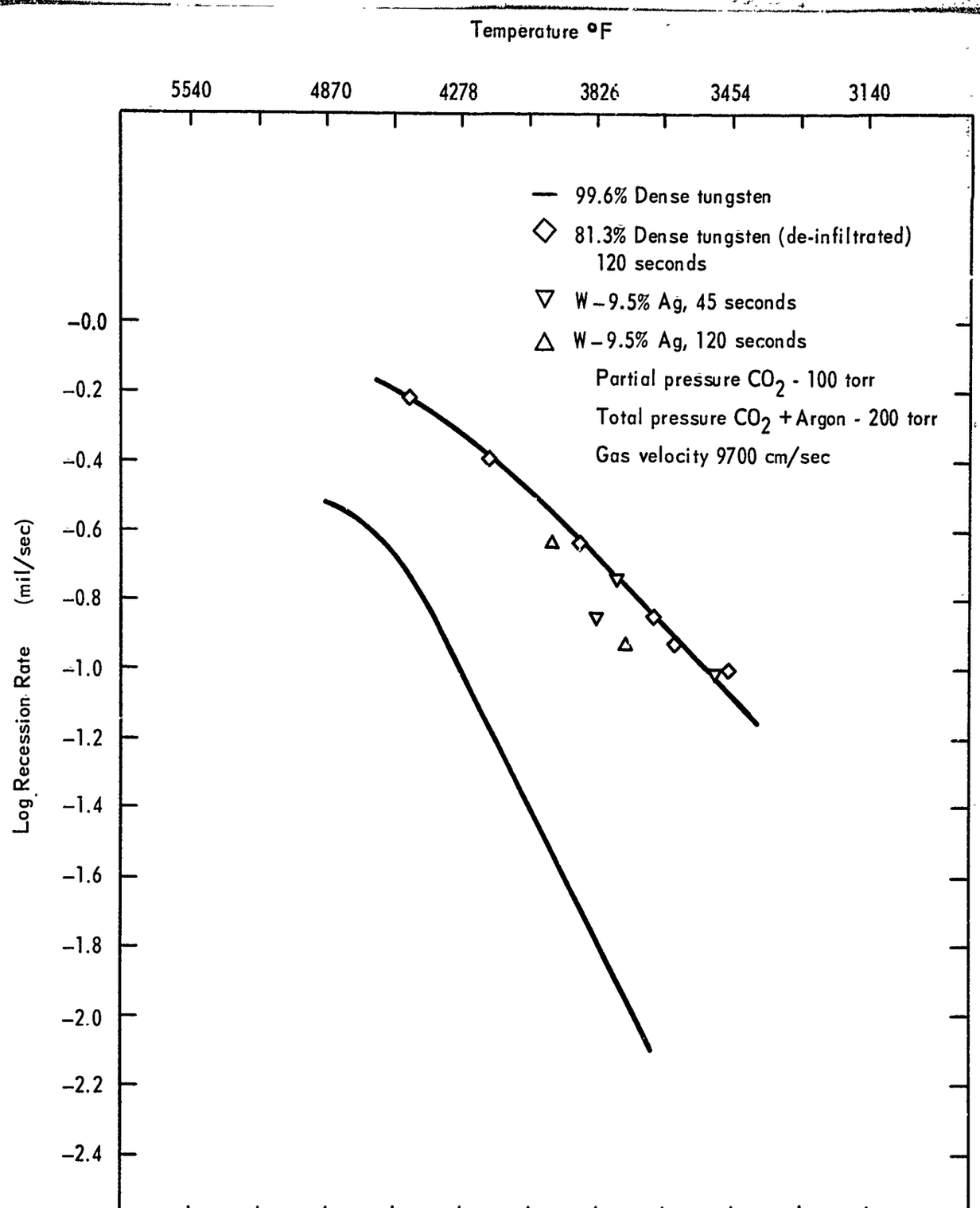

FIGURE B - 6 TEMPERATURE DEPENDENCE OF THE RECESSION RATE OF TUNGSTEN AND TUNGSTEN/SILVER IN CO_2

IV. RECENT PUBLICATIONS AND PRESENTATIONS

Presentations

"Nozzle-Wall Chemical Corrosion", R. W. Kebler and R. A. Graff. Presented at the Nozzle Heat Transfer and Erosion Meeting sponsored by the Solid Rocket Division of the Air Force Rocket Propulsion Laboratory, Edwards Air Force Base, California, September 1, 1964.

"Kinetics of the Oxidation of Tungsten by CO_2 above 2000°K", I. R. Ladd, J. M. Quets, J. E. Smith, R. A. Graff, and P. N. Walsh. Presented at the Symposium on High-Temperature Chemistry of the Chemical Institute of Canada, September 2-4, 1964 in Ottawa, Ontario.

"Electrical Properties of Some Transition Metal Carbides and Nitrides", John Piper. Presented at the International Symposium on Compounds of Interest in Nuclear Reactor Technology, Boulder, Colorado, August 3-5, 1964.

"Skeletal Refractory-Carbides and Metal Composites", R. W. Kebler, I. Binder, F. Keihn and I. R. Ladd. Presented at 21st Interagency Solid Propulsion Meeting, San Francisco, California, June 9-11, 1965.

"The CO_2-W Reaction: Interaction of Aerodynamics and Surface Kinetics", P. N. Walsh, R. A. Graff, J. M. Quets, I. R. Ladd and J. E. Smith. Presented at a Symposium on "Gas-Solid Reactions at High Velocity Flow Conditions" at the AIME Meeting, Chicago, Illinois, February 18, 1965.

"A Mass Spectrometric Study of the Oxygen-Tungsten Reaction", O. C. Trulson and P. O. Schissel. Presented at a Symposium on "Gas-Solid Reactions at High Velocity Flow Conditions" at the AIME Meeting, Chicago, Illinois, February 18, 1965.

"Mass Spectrometric Study of the Oxidation of Tungsten", O. C. Trulson and P. O. Schissel. Presentation at the National Bureau of Standards, November, 1964.

Research Reports

"Electrical Properties of Some Transition-Metal Carbides and Nitrides", John Piper, Research Report C-21, April 1964 - Contract DA-30-069-ORD-2787.

"Static Atomic Displacements Resulting From Vacancies in Defect Structures $TiN_x \square_{1-x}$", C. R. Houska, Research Report C-22, April 1964 - Contract DA-30-069-ORD-2787.

Research Reports Cont'd.

"Heat of Sublimation of Palladium", O. C. Trulson and P. O. Schissel, Research Report C-23, August 1964 - Contract DA-30-069-ORD-2787.

"Stagnation-Point-Velocity Distribution for a Compressible Fluid", R. A. Graff, Research Report C-24, October 1964 - Contract DA-30-069-ORD-2787.

"Mass Spectrometric Study of Zirconium Diboride", O. C. Trulson and H. W. Goldstein, Research Report C-25, October, 1964 - Contract DA-30-069-ORD-2787.

"Mass Spectrometric Study of the Oxidation of Tungsten", P. O. Schissel and O. C. Trulson, Research Report C-26, October 1964 - Contract DA-30-069-ORD-2787.

"The Elastic Properties of Polycrystalline Tungsten, 24°C-1800°C", R. Lowrie and A. Gonas, Research Report C-27, January, 1965 - Contract DA-30-069-ORD-2787.

"The Determination of Boron in Refractory Borides by Pyrohydrolysis", G. J. McKinley and H. F. Wendt, Research Report C-28, January, 1965 - Contract DA-30-069-ORD-2787.

"Methods of Analysis of Metal Refractories - Borides, Carbides and Nitrides of Hafnium Niobium, Tantalum, Titanium and Zirconium", R. E. Dutton, G. J. McKinley, D. McLean and H. F. Wendt, Research Report C-29, February, 1965 - Contract DA-30-069-ORD-2787.

Publications

"Thermal Expansion of Certain Group IV and Group V Carbides at High Temperatures", C. R. Houska, J. Am. Cer. Soc. 47, 310-311, (June 1964).

"High-Temperature Ductility of Large-Grained TiC", F. G. Keihn and R. W. Kebler, J. Less Common Metals 6, 484 (June 1964).

"Electrical Properties of Some Transition Metal Carbides and Nitrides", John Piper, Nuclear Metallurgy (AIME) 10, 29 (August 1964).

"Adsorption of Carbon Monoxide on Copper. Infrared Absorption Spectra and Thermodesorption", A. W. Smith and J. M. Quets, J. Catalysis 4, No. 2, p. 163-171 (April 1965).

"Low Critical Currents in Superconducting NbC", J. Piper, Appl. Phys. Letters 6, 183 (1965).

Publications Cont'd.

"Mass Spectrometric Study of the Vaporization of Palladium", O. C. Trulson and P. O. Schissel, J. Less Common Metals 8, 262 (1965).

"Mass Spectrometric Study of Vaporization Coefficients", O. C. Trulson and P. O. Schissel, in "Condensation and Evaporation of Solids", E. Rutner, P. Goldfinger and J. Hirth eds., Gordon and Breach, New York (1964).

"Mass Spectrometric Study of the Ti-B System", P. O. Schissel and O. C. Trulson, in "Condensation and Evaporation of Solids", E. Rutner, P. Goldfinger and J. Hirth eds., Gordon and Breach, New York (1964).

"A Mass Spectrometric Study of the Vaporization of Zirconium Diboride", O. C. Trulson and H. W. Goldstein, in "Condensation and Evaporation of Solids", E. Rutner, P. Goldfinger and J. Hirth eds., Gordon and Breach, New York (1964).

Union Carbide Corporation

Dr. A. L. Bayes

Mr. J. C. Bowman

Dr. J. C. Brantley/G. H. Clewett/
UCN Library

Dr. R. M. Bushong

Mr. M. C. Carosella

Dr. R. A. Charpie

Mr. D. E. Hamby

Dr. A. B. Kinzel

Helen F. Kuhns, Librarian
Union Carbide Stellite Div.

Dr. P. Lafayatis

Mr. W. Manly

Dr. R. W. McNamee

Dr. R. M. Milton

Dr. W. J. Spry (2)

Dr. Milton Stern

Mr. W. A. Steiner

Mr. H. F. Wendt/ Mr. A. L. Hallowell

Mr. H. L. Willard

Dr. C. E. Winters